A high-resolution reconstruction of climate variability at Lagoa Negra Lake Flores, Azores

UNIVERSITY
OF BERGEN

Master thesis in Quaternary Geology and Paleoclimate

Qaiser Hussain

Department of Earth Science
University of Bergen
February 2023

Abstract

This thesis has utilized four sediment cores LNG1, LNG2 1/2, LNG3, and LNG2 2/2 from Lagoa Negra lake Flores Island Azores for reconstruction paleoclimate. Climate variations occur on different time and spatial scales, from short-term fluctuations to long-term trends and from local to global. Climate change is expected to bring about global temperature increases, and changes in precipitation patterns. The cores were analyzed using radiocarbon dating, age-depth modeling, X-ray fluorescence, and hyperspectral imaging to determine variations in minerogenic influx and precipitation patterns. To better understand regional climate variability, it has been compared with other North Atlantic climate reconstructions NAO_{Trouet} (2009) and NAO_{Ortega} (2015). Radiocarbon dating is used for sediment chronology and age-depth modeling shows the age extends to 1290CE. Furthermore, XRF and Hyperspectral Imaging have been used for the determination of minerogenic influx.

The Lagoa Negra records suggest that the variations in Ti reflect the minerogenic influx. High values of Ti are considered to be high sediment influx and replicate high precipitation. On the other hand, the Inc/Coh replicates the organic matter.

It has been found that analyzed elements showed variations over time which have been linked with climate changes. Analysis of sediment cores from the lake indicates that during the period from 1291 CE to 1400 CE, 1450CE to 1600CE, and 1700CE to 1800CE there was a low minerogenic influx, and low precipitation could replicate positive NAO. Whereas high Ti values represent 1450CE, 1600CE-1700CE, and early 1800CE, which could be phases of high precipitation and negative NAO.

Acknowledgment

First and foremost, I would like to express my sincere gratitude to my supervisors Willem G.M. van der Bilt, and Benjamin Aubrey Robson, for their guidance, encouragement, and support throughout my academic journey. Their unwavering patience, expertise, and knowledge have been instrumental in helping me complete this thesis.

I would also like to extend my appreciation to the faculty members of Earth Science, for providing me with a strong foundation. Their teachings and mentorship have been instrumental in shaping my academic and professional growth.

I am grateful to the staff of the EarthLab University of Bergen, who provided me with the necessary resources and support to conduct my research. Their assistance and collaboration have been invaluable.

I would like to express my gratitude to my family for their love, encouragement, and support throughout this journey, and I would also like to extend my appreciation to my friends, Violeth Swai, Waqas Hussain, and Zain Ul Abideen, for their valuable contributions. Their motivation and belief in me have been a source of strength and inspiration.

Finally, I would like to thank all participants who took part in this study, for their time and willingness to share their information. Their contribution has been essential to the success of this research

Contents :

1 Introduction and motivation

Climate variations occur on all temporal and spatial scales, from short-term fluctuations to long-term trends, and from local to global. Climate change, as predicted by most current models, is expected to bring about an increase in global temperatures, changes in precipitation patterns, and rising sea levels. Temperature increases are likely to be greater on land than in oceans and more pronounced in inland regions compared to coastal areas and in polar regions compared to the tropics. Precipitation patterns are expected to be more complex, and largely dependent on factors such as the proximity to water bodies, mountain ranges, and wind flow direction. In general, most models predict an increase in precipitation in areas near the polar regions and a decrease in areas near the tropics. Additionally, rainy seasons in tropical regions are expected to see an increase in precipitation (Koetse & Rietveld, 2009). The North Atlantic Oscillation and the El Nino are the main two patterns contributing to large climate variations (Andrade et al., 2008). The North Atlantic Oscillation (NAO) is a fluctuation in atmospheric pressure between the subtropical anticyclone near the Azores and the subpolar low-pressure system near Iceland. It plays a significant role in determining the variability of atmospheric circulation patterns on a seasonal to interdecadal time scale, not only in the North Atlantic region but also worldwide (Pinto & Raible, 2012). To assess the state of NAO, the North Atlantic Oscillation (NAO) index is used, which is a measure of the difference in atmospheric pressure between the Icelandic Low and the Azores High. The index is calculated by subtracting the normalized sea level pressure at Reykjavik, Iceland from the normalized sea level pressure at Ponta Delgada in the Azores, Gibraltar, and Lisbon, Portugal. A positive index indicates that the pressure difference is stronger than normal, and a negative index suggests that the pressure difference is weaker than normal. The NAO index is widely used as a measure of the North Atlantic Oscillation, as it is closely related to the variability of the atmospheric circulation patterns in the North Atlantic region, and is frequently used as a general indicator of the strength of the westerly winds over the eastern North Atlantic and western Europe, particularly during the winter season. It is considered a key factor in determining the winter climate in Europe. (Wanner et al., 2001). The North Atlantic Oscillation (NAO) has been identified as the primary large-scale pattern that impacts the climate of the Azores Archipelago at interannual time scales. This can control various mechanisms such as tropical cyclones, thunderstorms, and sea surface temperature anomalies, which bring moisture and contribute to various weather phenomena (Hernández et al., 2017), and can have significant impacts on regional and global climate, including temperature, precipitation, and wind patterns. (Hurrell & Deser, 2010). To understand

climate variabilities and patterns, paleoclimate variabilities are vital to study (Powers et al., 2004). The intricate relationships between physical, chemical, and biological processes underlie the climate-driven change in a lake (Meyers & Lallier-Vergès, 1999). For understanding the climate, most of the records can be utilized, like tree rings, historical documents, marine and lake sediments, ice cores, and corals (Bradley, 1999). The reconstruction of past climate conditions is a way to understand how climate has varied over time. Lake sediments are a valuable resource in this regard as they offer a continuous record of environmental changes that can be used to reconstruct climate (Mason et al., 1994). It can preserve potentially high sediments which are being utilized for reconstructing past climate patterns and understanding how the lake has changed in response to shifts in climate. crater lakes are one of the main focuses of paleoclimate research (Barr et al., 2014). The sediments from these crater lakes can provide information about the origin, weathering, and climate change, furthermore, they preserve different properties and indicators like physical, chemical, and biological (Nguetsop et al., 2013), also mineralogy and geochemistry. Geochemical variations in sedimentary records can be used to detect changes in the balance between evaporation and precipitation, which reflects regional climate. The rate of chemical sedimentation is affected by the relationship between water input (runoff, precipitation) and water loss (evaporation). These variations in the sedimentary record can be used to infer changes in the dynamics between evaporation and precipitation and regional climate (Adrian et al., 2009). Besides these, the organic matter and the total organic carbon in lacustrine sediments are indicators of the physical and chemical properties which is used for the study of the paleoenvironment (Ekoa Bessa et al., 2021).

The motivation behind this study is to reconstruct and gather information on past climate variability using sediments from the archipelago`s volcanic Maar lakes Lagoa Negra (Figure 1). Lagoa Negra lake is located on Flores Island Azores (Báez et al., 2021) in the North Atlantic Ocean (Figure 1). Finely laminated three cores extracted, have been studied and used a combination of different approaches to reconstruct past climate variability.

The study hopes to provide valuable insights into how past climate variability has impacted the region and to better understand the mechanisms driving these changes. The results of this thesis may also have implications for understanding current and future climate patterns in the region.

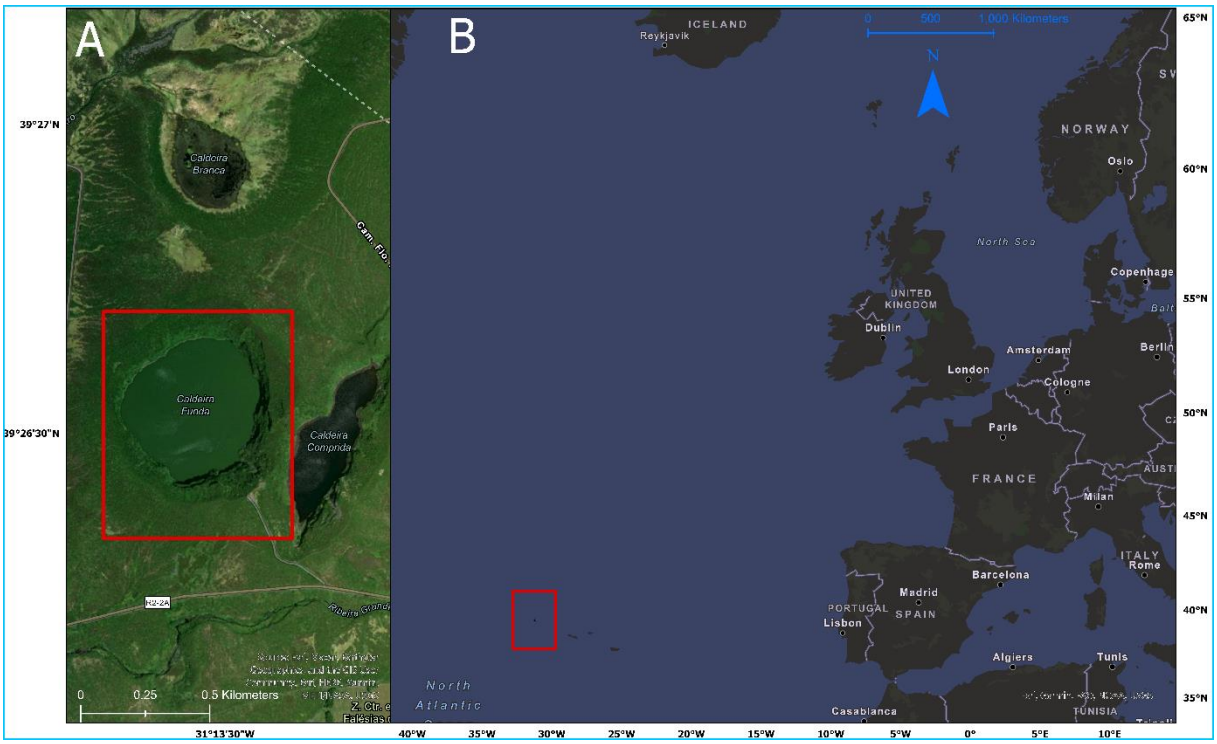

Figure 1: Location Map of the study area “Lagoa Negra” one of the archipelago`s Maar lakes, North Atlantic Ocean. A) Lake Lagoa Negra in the Flores Island. B) visual representation of the North Atlantic Ocean showing the study area in Azores Archipelago has been marked

2 Background

2.1 Study Area

Flores, which is a small island, comprises 142 km² located in the North Atlantic Ocean (Figure 1), and it is a part of the Azores Archipelago which emerged because of volcanic activities and constitutes the western part of the Azores Archipelago. The Azores archipelago consists of nine volcanic islands (Santos et al., 1995). These islands are divided into western, eastern, and central groups. The western group comprises the Corvo and Flores, while Sao Miguel and Santa Maria lie in the Eastern group, lastly, the central group has Faial, Pico, Graciosa, Sao Jorge, and Terceira. Out of these islands, the largest island is Sao Miguel which comprises 745km² while Corvo is the smallest island with 17km². Flores island is 142km². Pico with 2351m elevation above sea level categorized as the highest elevation, while Graciosa with 402m is the lowest elevation point. The other five islands have an elevation of around a thousand meters, with which Flores has 915m highest elevation above sea level (Borges et al., 2009). Flores Island experiences lower temperatures because of the orography. The average temperature in Flores is 17.8° and the annual precipitation is 1430mm (Rodrigues & Antunes, 2014). The Lagoa Negra Lake is located in the central-western part of Flores Island. The bathymetry of the lake indicates that it is 110m deep (Figure 4), which is the deepest lake on Flores Island (Rodrigues & Antunes, 2014).

2.2 Regional Geology

Flores Island along with Corvo Island mounts in the junction of triple plates namely Eurasian, North America, and African plates (Figure 3). The island lies in the North American plate on the axis of the Mid-Atlantic Ridge towards the west approximately 100km (Genske et al., 2016) Mid Atlantic Ridge influenced the western part and because of this making north-south striking tectonic structure (Métrich et al., 2014). The island formed 2.5 Ma ago in the late Pliocene (Andrade et al., 2021). Flores island has complex geology that constitutes the vertical movements resulting the mass wasting (Hildenbrand et al., 2018), and affecting the crustal region which is continuing since 1Ma, along with the submerged island constitutes the tectonic evolution. But this has been dominated by the Flores Island uplifting because of isostasy (Azevedo & Ferreira, 2006).

The Central Plateau of the Island is a 500m above sea level upland central area characterized by the topography of the island, covered by valleys and steep slopes (Andrade et al., 2021).
Geologically around 20-36 Ma made the old volcanic plateau in the Azores (Borges et al., 2009) According to Andrade et al (2021), there are three stages of volcanic activity on the island. In the first stage, the volcanism was comprised the explosive events, which happened around 700 – 500 ka. The second stage called the intermediate stage had a gusher eruption. This stage occurred in 400 – 200 ka. The final stage occurred in 3 – 2.9ka had the strombolian eruption and the phreatomagmatic activity.

The volcanic activities in Flores Island constitute basaltic and hawaiitic lavas, which are because of different processes and eruptions. There are two major complexes grouped according to deposits and volcanic lavas. The first one is called the Basic Volcanic Complex (BC). The BC is involved in a submarine and emergent volcanism that resulted in different structures. Secondly, the UC Upper volcanic Complex has all the structures associated with subaerial volcanic activities (Azevedo & Ferreira, 2006). The vents which are made by the volcanic activities are divided into two clusters. The first one which comprises different lakes namely Lagao Negra, Lagao Comprida, Lagao Seca, and Lagao Branca are put in the Northern vents. These vents are linked to N25°E and N – S fractures. While the remaining two lakes Lagao Funda and Lagao Rasa have steep slopes and depth and are categorized as part of the southern cluster (Andrade et al., 2021).

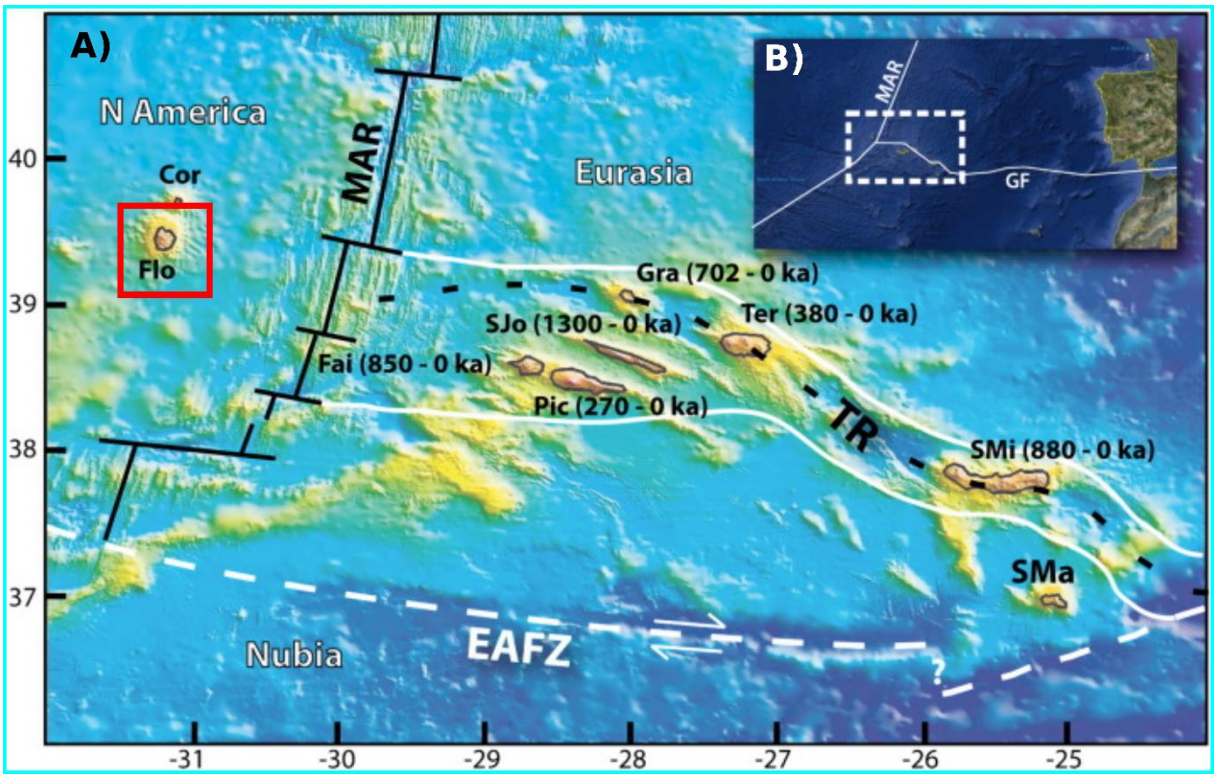

Figure 2: Regional geology. A) Study area Flores Island marked B)represents Azores Archipelago marked (França et al., 2003)

2.3 Climate

The Azores Archipelago's climate is primarily influenced by the strength and location of the Azores Current, a branch of the Gulf Stream, and the Azores Anticyclone, a high-pressure system that moves seasonally. When the high-pressure system is positioned over the islands during the summer, it leads to relatively dry and sunny conditions. The western islands of the Azores receive the highest average annual rainfall, while the eastern islands have lower precipitation and a more pronounced dry season. These climate patterns are caused by the Azores Current and Anticyclone, which control the temperature, wind direction, and precipitation over the islands (Connor et al., 2012). Due to subtropical high pressure, it faces a humid subtropical climate (Rodrigues & Antunes, 2014). Two seasons can be prominent, a humid season and the second one is a dry season. The humid season encounters high precipitation from September to March. The precipitation from September to March constitutes an average of 112mm per month, while an average of 59 mm of precipitation occurred in other months (Richter et al., 2022).

The pressures can be determined in different stations in the Azores high and Icelandic low, which is due to the North Atlantic Oscillation. The westerlies are blowing across the North Atlantic Ocean between the Azores and Iceland. In the winter season, the westerlies become

more intense (Sarachik et al., 2000). When the pressure of sea level is above normal over the Azores and below over Iceland, then the North Atlantic Oscillation NAO is considered to be of high index (Iqbal & Rashid, 2016).

According to Báez et al (2021), Europe experiences different types of winter. When the NAO is positive, the Azores and southwestern Europe have high pressure, whereas Iceland has low pressure. Northwestern Europe experiences high temperatures. Besides this, in the northern mid-latitudes, NAO+ produces above-average westerly winds and in the Mediterranean region, the climate becomes dry. While in the other phase when the NAO is negative, the situation is reversed and produces precipitation in southern Europe (Figure 4).

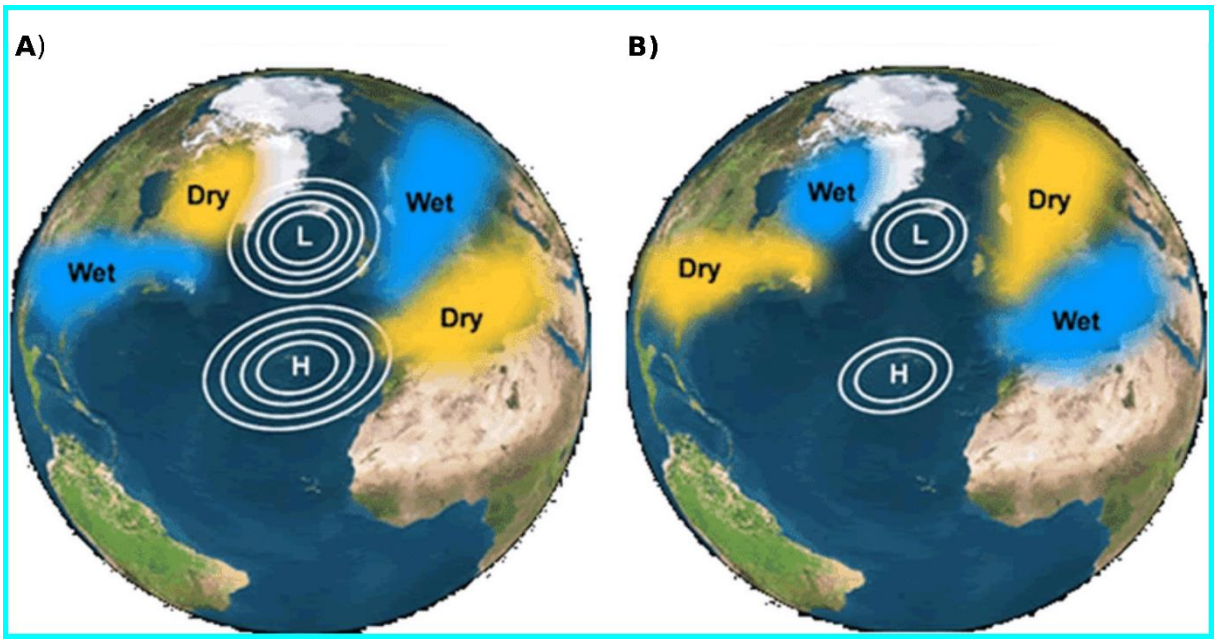

Figure 3: Schematics of the A)Positive B) negative phases of North Atlantic Oscillation NAO indicating A) when NAO is positive Flores Azores experiences dry B) and wet weather when its NAO negative (Hosseini et al., 2022)

3 Materials and Methods

3.1 Coring

All the investigated sediments were extracted using a Uwitech gravity corer in September 2021 from Lagoa Negra Lake Flores Island Azores (Figure 1).

3.2 Sample preparations

For laboratory analyses, the EARTH LAB of the earth science department at the University of Bergen has been used. All the multi-proxy analyses have been carried out here. The cores are split into two halves, the work, and reference halves. The cores have been marked with the depth scale, wrapped the cores with protector sheets, and stored in the cold section.

3.3 Sampling for Radiocarbon C-14 dating

Radiocarbon dating is a method of determining the age of organic materials by measuring the radioactivity of the carbon-14 isotope that is present in the material. The technique is based on the fact that 14C is produced in the Earth's atmosphere and absorbed by living organisms, and that it decays at a known rate after the organism dies (Hajdas et al., 2021). In this study, we used radiocarbon dating to determine the age of samples, that have been taken from LNG2 2/2 and LNG2 1/2 sediment cores. Altogether four samples were collected and rinsed with distilled water through sieves. These samples were then studied through a microscope and plant remains have been collected from each sample in sufficient amounts and put in the containers. These containers are then put under 50°C to become dry. Lastly, the samples were sent to Poznań Radiocarbon Laboratory Poland.

3.4 Grain Size Analysis

Grain size analysis has been applied on LNG1, LNG2 1/2, and LNG2 2/2. From each sediment core, multiple samples have been collected. To determine grain size distribution samples have been mixed with a combination of water and a chemical called 14Calgon to create a suspension. The suspension have been then shaken to ensure that all the particles in the sample were evenly dispersed and in suspension. Once the suspension becomes ready, the grain size analysis has been performed using a Mastersizer 3000 from Malvern Instruments Ltd. This is a specialized instrument that uses laser diffraction to measure the size of individual particles in a suspension. The laser light is passed through the suspension and the scattered light is collected and analyzed

to determine the size of the individual particles. The instrument then provides information about the particle size distribution of the sample, including the D10, D50, and D90 values (Ryżak & Bieganowski, 2011).

3.5 ITRAX: X-Ray Fluorescence core scanner

Geochemical profiles in sediment cores can reveal the environmental history of a lake. Elements such as Titanium Ti can be used to determine the extent of external input in the lake (Anderson et al., 2018). The µ-XRF core scanning allows for the quick acquisition of continuous sub-millimeter profiles of elemental variation and can be used to detect changes in geochemical relationships that are influenced by temperature and precipitation, and thus has great potential for understanding how lakes have responded to past climate conditions.

The ITRAX has powerful capabilities that can scan element variations with high resolution, as well as provide optical imaging, and can be performed on sediment cores and rocks. The core should be split into two halves and the length can be a maximum of 1800 mm. while the diameter can be from a few cm to 12 cm (Croudace et al., 2006). The XRF is working on the principle that the primary photons of suitability are bombarded, which stimulates the sample photoelectric fluorescence of the characteristics of secondary X-rays (Boyle, 2000).

On four cores namely LNG1, LNG2 1/2, LNG2 2/2, and LNG3 the XRF was carried out. The split cores were put horizontally onto a cradle. The top of the cores is positioned towards the right. After putting the cores, scanning is initiated, and defined the length of the core. The defined length for the LNG1 core is 61.96cm, and for LNG2 1/2, is 43.02cm, whereas the LNG2 2/2 is scanned in two parts, LNG2 2/2a and LNG2 2/2b. The length for LNG2 2/2a is 73.98cm and 75.98cm and finally, the LNG3 length is 35.48cm. The resolution for scanning is set to 200µm. The counting time of the scan has been set to 10 s. The Chromium (Cr) tube is used for the analysis, as it has a high atomic number, which can be a good emitter of X-ray, and also has a high melting point, which can make it resistible to high temperatures during X-ray emission. The surface topographic scan was then initiated. Approximately after 5 minutes, the core returned back and before starting the scan again, some adjustments were made like adjusting the parameters and defining the elements. Furthermore, in batch analysis mode the names of the core were given, and reviewed the count times, and scan limits, and then started the scan. The scan normally took 6 to 8 hours on each core. After scanning is complete, out of the spectrum the elemental peak areas have been extracted. For this Q-Spec spectral analysis software is used.

3.6 Hyperspectral Imaging

A recently created, non-destructive, and real-time spectroscopic imaging technology called hyperspectral imaging (HSI) gives quantitative information on the visible and near-infrared spectrum of sediments core (Van Exem et al., 2018). Comprehensive sediment core analysis and the interpretation of climate proxy data are made possible by the procedure, which allows the measurement of hundreds of spectral bands with high resolution at small scales ranging from micrometers to nanometers (Rein & Sirocko, 2002). For many years, techniques that use reflectance in the "visible to near-infrared range" (VNIR) have been utilized for logging color on geological sediment samples, using color spaces. These techniques have been further developed for specific identification and interpretation of different materials and species. With the help of a hyperspectral camera that can scan complete split cores at a high resolution and be used to distinguish between biogeochemical compounds and single elements in the VNIR region. The scanning camera is employed to assess the photosynthetic portion of sediment by capturing a high-resolution image (measured in micrometers or nanometers), that acquires the spectral information from the surface of the sediment, his precise and continuous measurement of the image wavelengths generates a full spectrum for every pixel of the acquired image, which can then be utilized for identifying materials with similar spectral properties (Shippert, 2003). HSI uses its understanding of the interactions between substances and various wavelengths, as well as determining the energy absorbed in the spectrum to identify diagnostic absorption bands. A time series of relative absorption band depths (RABD), based on the unique diagnostic absorption wavelengths of particular materials, are created during the acquisition of a spectral map of a sediment core (Butz et al., 2015). To detect sedimentary components and properties like organic matter, sedimentary structures, minerals particle size, and sedimentary pigments, HSI can be utilized by using the wavelengths of visible and near-infrared (VNIR; 400–1000 nm) and short wave infrared (SWIR; 1000–2500 nm) (Zander et al., 2022). Following (Butz et al., 2015) all the cores LNG1, LNG2 1/2, LNG2 2/2, and LNG3 were processed for spectral analysis using the SCS sediment core scanning system, which is developed by Specim Ltd at earth lab University of Bergen. The camera was set accordingly. Its field of view (FOV), focus, frame rate, and speed of the sample tray moving were optimized. Target start and stop were set for each core separately. Furthermore, image correction was done for white and dark references. Preprocessing is done and the Region of Interest (ROI) has been defined. After preprocessing, postprocessing is carried out, which is discussed in chapter 4.

4 Results

4.1 Coring

Three cores LNG1, LNG2, and LNG3 have been extracted from Lagoa Negra Lake. The lake comprises 110cm in depth (Figure 4). The LNG2 has been divided into two parts called LNG2 1/2, and LNG2 2/2. The LNG1 comprises a total length of 61.96cm, LNG2 is 187.98cm in the top portion, LNG2 1/2 is 43.02cm, and LNG2 2/2 has a length of 144.96cm.

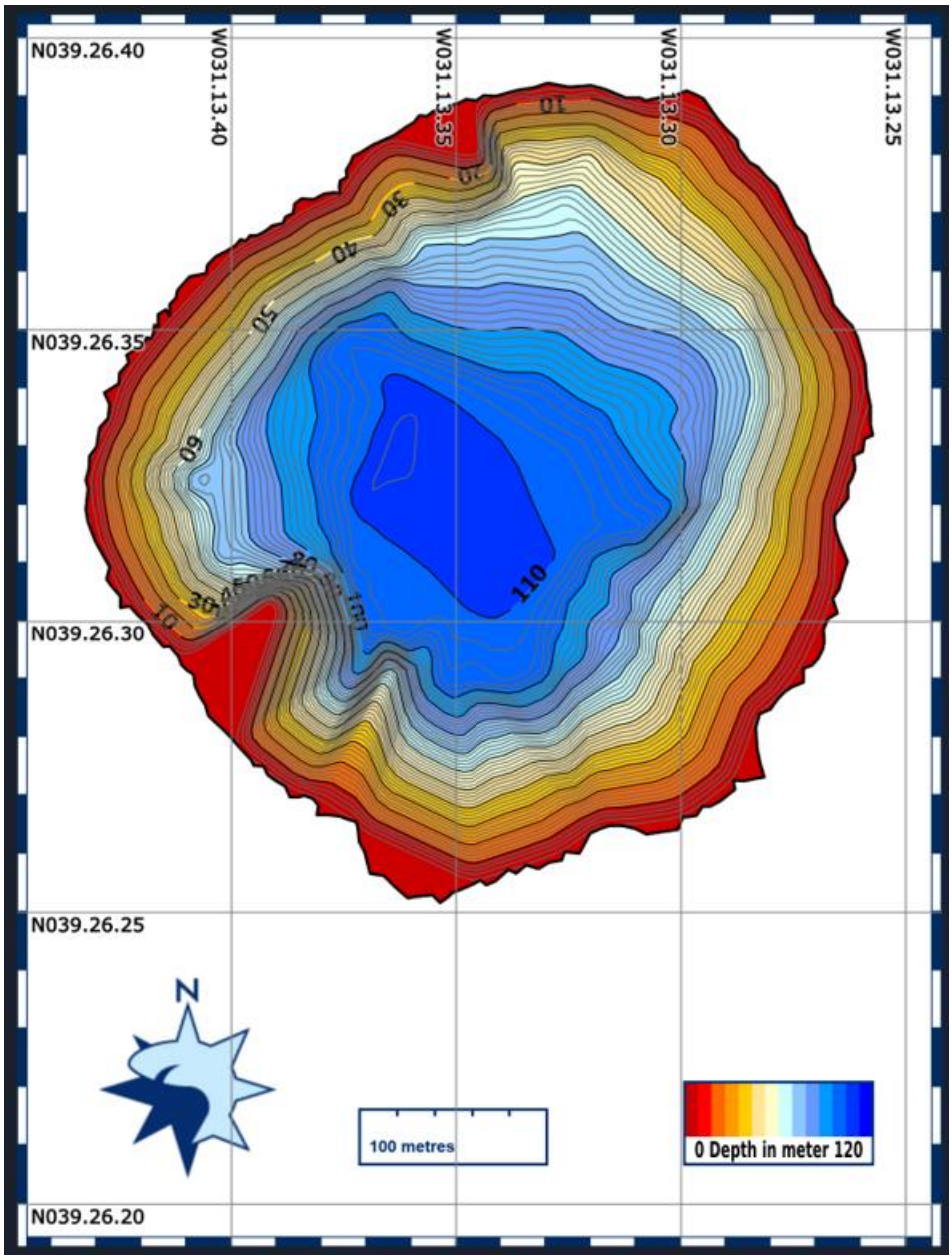

Figure 4: Bathymetry map of the study area represents the depth of Lago Negra Lake, which comprises 110m.

4.2 Lithological core descriptions

The cores collected from Lagoa Negra Lake have been arranged in a specific sequence to create a comprehensive view of the data collected. The red box in Figure 5 highlights the overlap of the cores LNG1, LNG3, and LNG2 1/2, which indicates the presence of similar or related information in these cores. The yellow box represents the correspondence between cores LNG1 and LNG2 1/2, implying that there is a clear connection between these two cores and their respective data sets. This organized arrangement of the cores provides a clearer understanding of the information gathered from the lake and can help in further analysis and interpretation

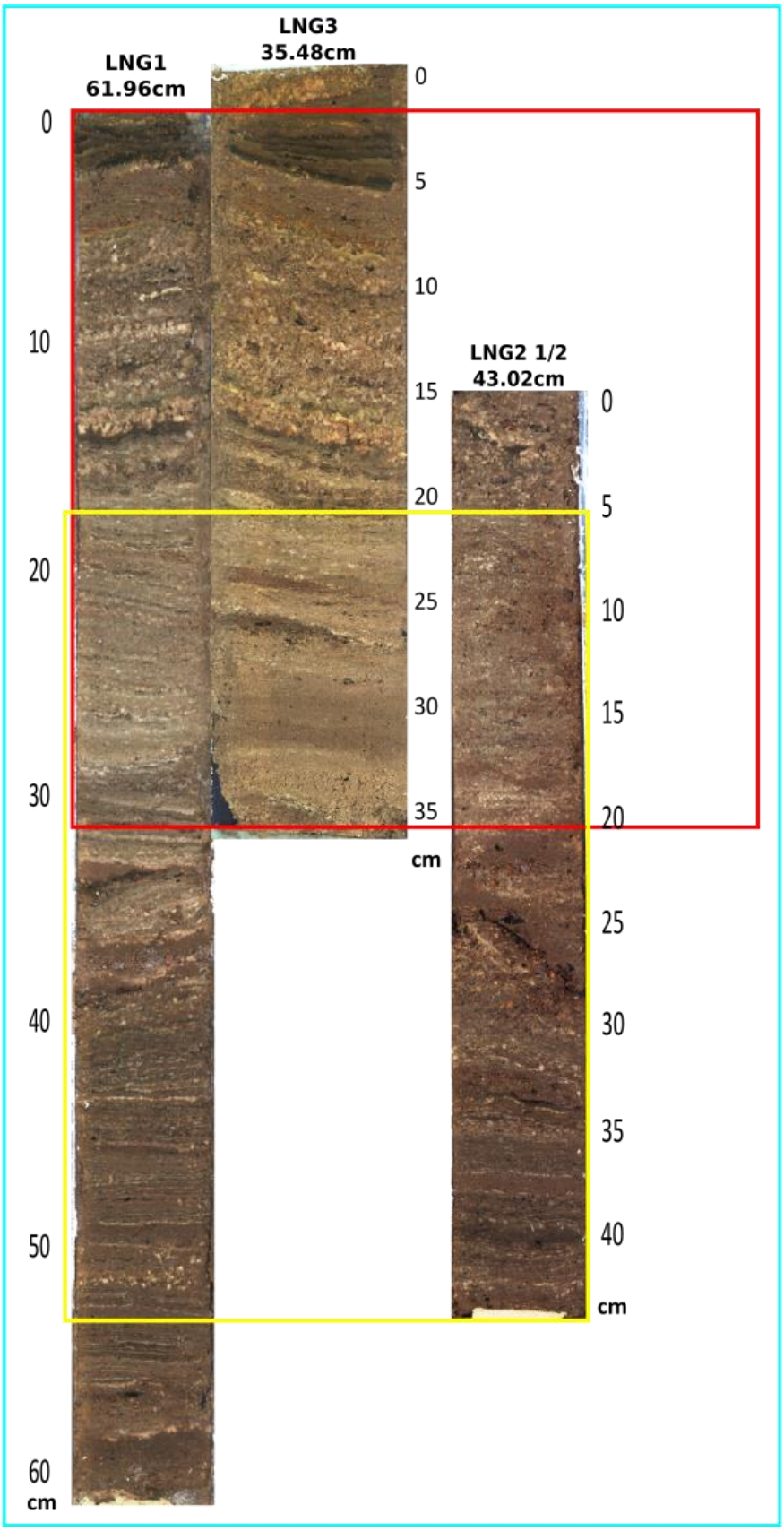

Figure 5: All the tree cores have been aligned based on the same lithology. The red box shares LNG1, LNG3, and LNG2 1/2 overlapping, while yellow box comprises LNG1 and LNG2 1/2

The cores have been divided into five units A, B, C, D, and E (Figure 6) based on visual logging. Unit A, which consists of LNG1 and LNG3, has dark brown fine silty sand that is characterized by its fine texture and dark color. This type of sedimentation is commonly found in areas with considerable amounts of organic matter and low levels of water flow.

Unit B is characterized by light brown color, and it comprises of very fine to fine silty sand. This type of sedimentation is common in areas where water flow is low, and there is a high presence of fine particles.

Unit C, which encloses all the tree cores LNG1, LNG3, and LNG2 1/2, is a light brown to yellowish color and has a sedimentation range from medium to coarse sand. This type of sedimentation is typically found in areas with higher water flow, and the medium to coarse sand particles suggest a higher energy environment.

Unit D is comprised of very fine to fine silt and has a light to yellowish color. This type of sedimentation is commonly found in areas with low water flow, where the fine silt particles are able to settle and accumulate.

Unit E, found in LNG1 and LNG2 1/2, is characterized by a dark brownish color with coarse to fine silty sand. This type of sedimentation is typically found in areas with high water flow, where the coarse to fine silty sand particles have been transported and deposited. Additionally, lamination can also be seen in cyclic manner with alternating layers. This cyclic pattern is typically formed due to changes in water flow and sediment supply, leading to the formation of distinct layers that reflect the different conditions at the time of deposition.

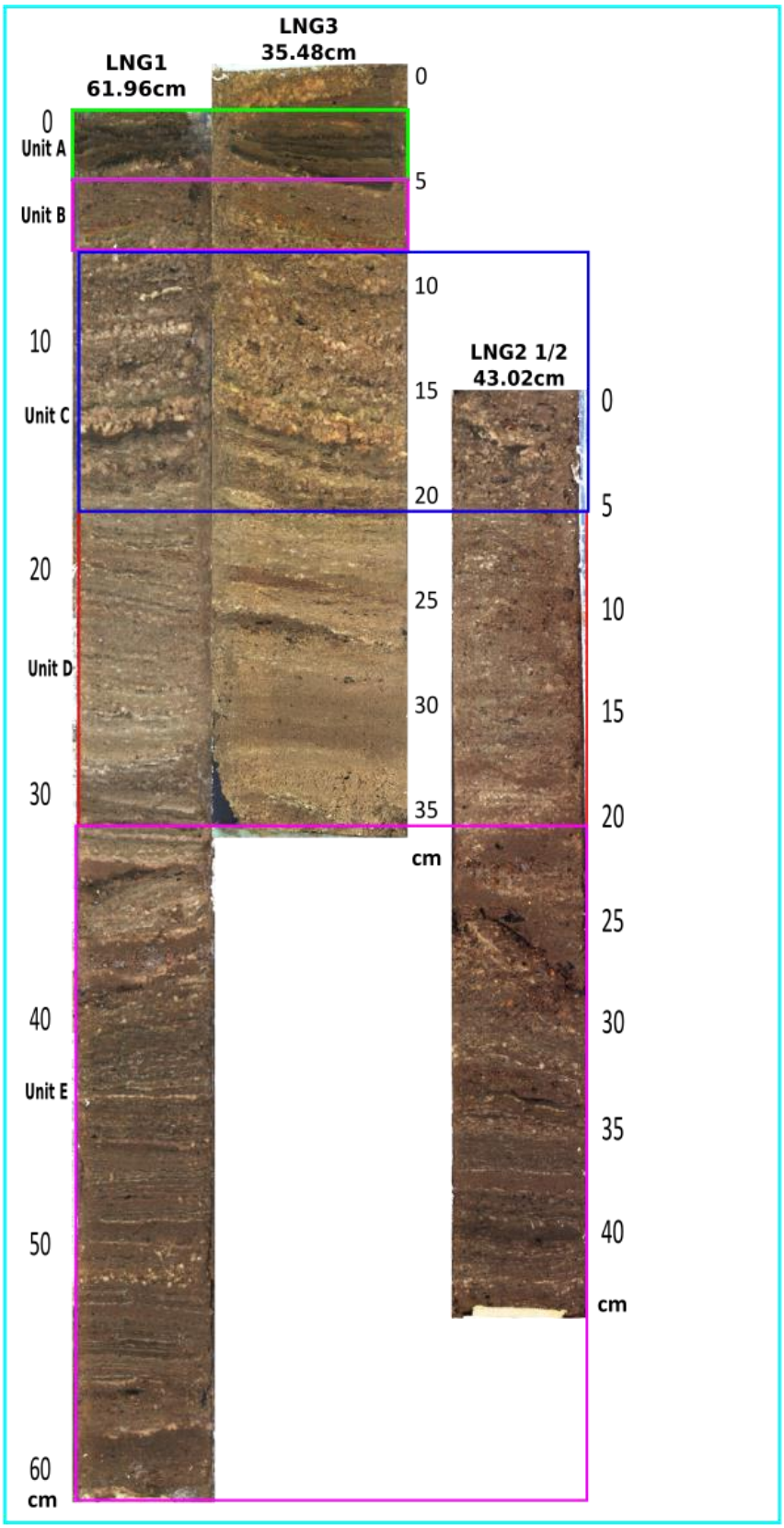

Figure 6: shows all the tree cores aligned which overlap and share the same stratigraphy and are divided into different units based on visual analysis and lithology. Unit A and B comprises LNG1 and LNG3, Units C and D cover all the three cores LNG1, LNG2 1/2 , and LNG3, while Unit E comprises LNG1 and LNG 2 1/2

The information provided in Figure 7 and Figure 8 from the Gradistat obtained from grain size analysis shows the average sediment composition of LNG1 and LNG2 1/2 respectively. LNG1 is comprised of silty sand, with an average of 51.7% sand and 48.3% silt. On the other hand, LNG2 1/2 is comprised of sandy silt, with 42.8% sand and 57.2% silt. These data provide valuable information on the texture of the sediment in each location and can be used to understand the depositional environment and processes that have shaped the landscape. The different percentages of sand and silt can be used to infer differences in water flow, energy levels, and sediment supply, among other factors. For example, the higher percentage of sand in LNG1 compared to LNG2 1/2 may suggest higher energy levels or a greater supply of sand-sized particles in the depositional environment. On the other hand, the higher percentage of silt in LNG2 1/2 compared to LNG1 may indicate a different depositional environment with lower energy levels or a greater supply of silt-sized particles.

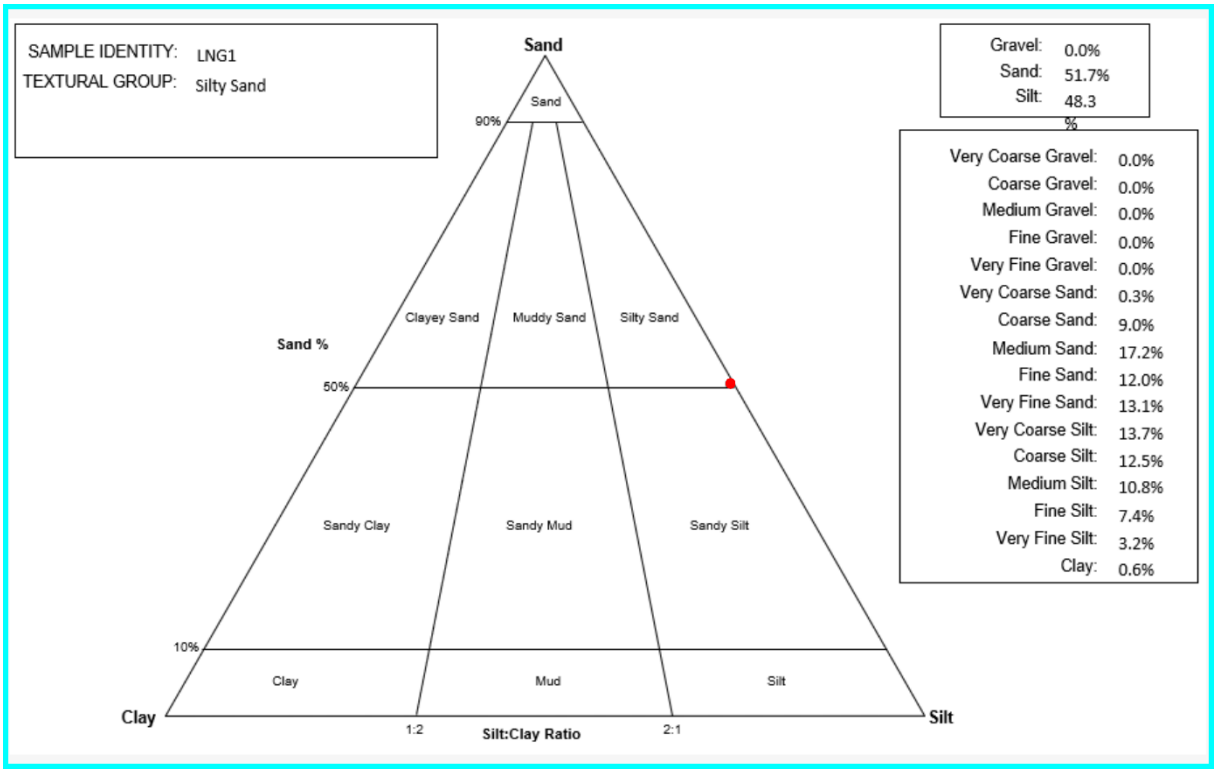

Figure 7: Shows GRADISTAT result of the grain size distribution of LNG1. The red dot shows the average of the samples being used.

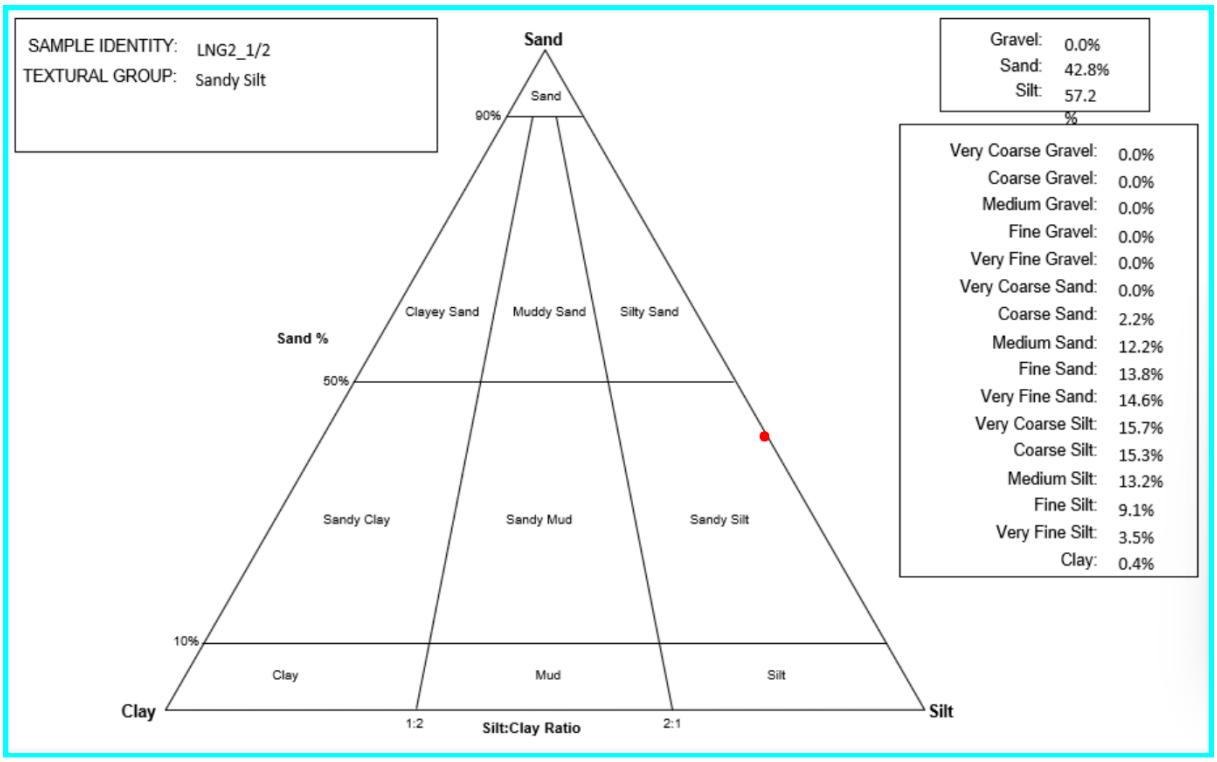

Figure 8: Shows Shows GRADISTAT result of the grain size distribution of LNG2 1/2. The red dot shows the average of the samples being used.

The LNG2 2/2 sediment core (Figure 9) is a finely laminated sediment core that was separated from the LNG2 1/2 core (Figure 5). The core is 144.96 cm in length and has a light yellowish to dark brown color, with the upper portion being light brown and the lower portion being dark brown. In some areas, yellowish-brown laminations can also be seen in the core.

The sediment composition of LNG2 2/2 is predominantly silty sand, with 62.6% sand and 37.4% silt (Figure 10). The high proportion of sand in the sediment indicates that the depositional environment was characterized by moderate to high water flow and energy levels, which allowed for the transportation and deposition of sand particles. The presence of silt in the sediment suggests that the depositional environment was also characterized by low energy levels and quiet water, which allowed for the finer particles to settle out of the water column and become incorporated into the sediment.

The laminations in the core are indicative of cyclic changes in the depositional environment, with different sediment types and colors being deposited at different times. These changes can be used to infer changes in water flow, energy levels, sediment supply, and other factors that have shaped the depositional environment over time.

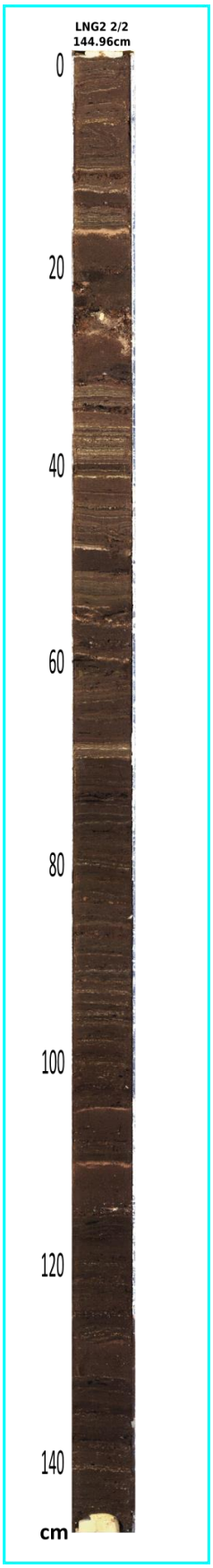

Figure 9: Represents fine lamination of the sediment core LNG2 2/2. The core comprises 144.96cm in length

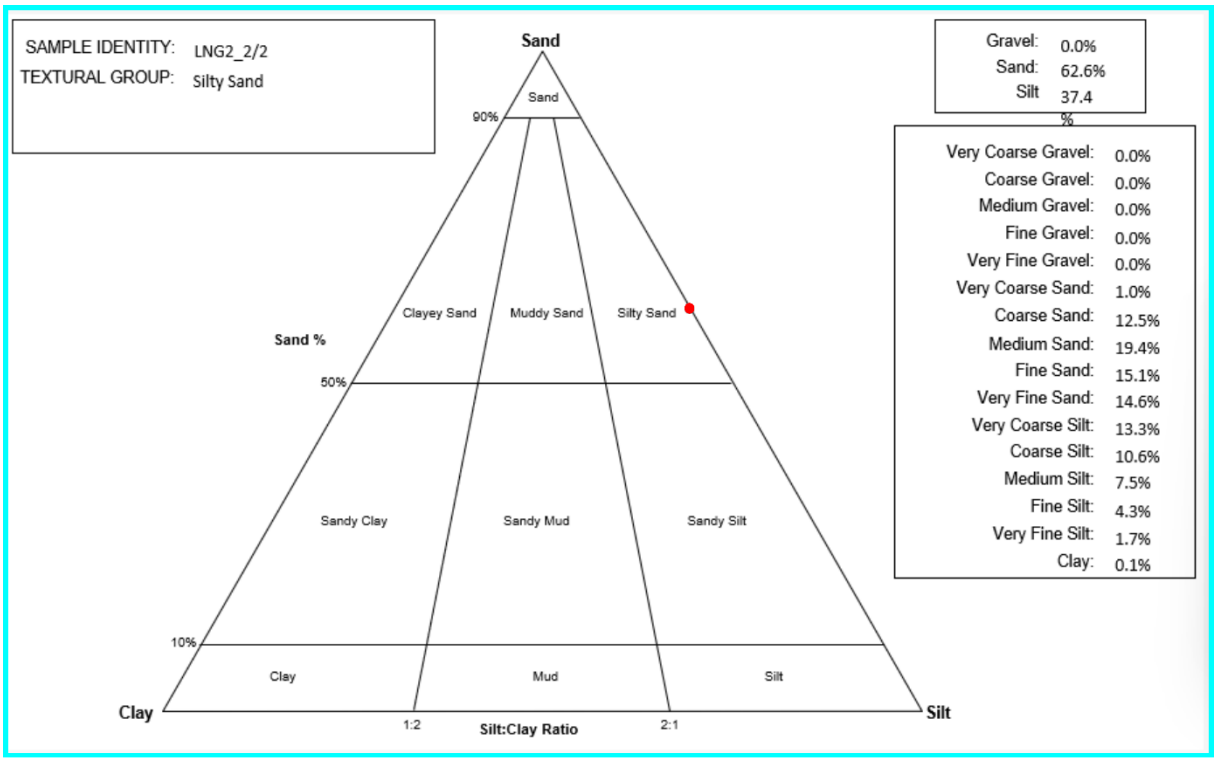

Figure 10: Shows Shows GRADISTAT result of the grain size distribution of LNG2 2/2. The red dot shows the average of the samples being used.

4.3 Radiocarbon dating

Four samples of the plant remains from sediment cores LNG2 2/2 and LNG1 of Lagoa Negra lake Azores Portugal are extracted, processed, and sent to Poznań Radiocarbon Laboratory Poland for radiocarbon dating.

Core	Sample name	Depth	Lab. no	Material	Uncalibrated ^{14}C ages (BP)
LNG2 2/2	S1	144	Poz-136042	Plant remains	**600 ± 30 BP**
LNG2 2/2	S2	77	Poz-136043	Plant remains	**400 ± 30 BP**
LNG2 2/2	S3	35	Poz-136077	Plant remains	**305 ± 30 BP**
LNG2 1/2	S4	30	Poz-136078	Plant remains	**130 ± 30 BP**

Table 1: Radiocarbon dating C-14 results conducted by Poznań Radiocarbon Laboratory Poland, samples from sediment cores LNG2 2/2 and LNG2 1/2

4.4 Age model

For age-depth modeling Oxcal program using Bayesian statistics methods (Bronk Ramsey, 2021) is used, and is calibrated with InCal 20 (Reimer et al, 2020) (Figure 11) which provided a probability distribution for the calibrated ages of our samples (Table 2). The results from the OxCal analysis allowed us to make precise and accurate inferences about the ages of our samples and the context of their deposition.

Core	Sample name	Depth LNG2 2/2, LNG2 1/2	Depth LNG2	Lab. no	Material	Uncalibrated ^{14}C ages (BP)	Calibrated Age Range (yrBP) 95.4% Probability	Calibrated Age Range (CE) 95.4% Probability
LNG2 2/2	S1	144	187	Poz-136042	Plant remains	600 ± 30 BP	658-556	1291-1395
LNG2 2/2	S2	77	120	Poz-136043	Plant remains	400 ± 30 BP	482-426	1469-1524
LNG2 2/2	S3	35	78	Poz-136077	Plant remains	305 ± 30 BP	388-318	1562-1632
LNG2 1/2	S4	30	30	Poz-136078	Plant remains	130 ± 30 BP	287-188	1664-1762

Table 2: Radiocarbon dating C-14 conducted by Poznań Radiocarbon Laboratory Poland, samples from sediment cores LNG2 2/2 and LNG2 1/2 and calibrated age using InCal 20 based on Bronk Ramsey, 2021.

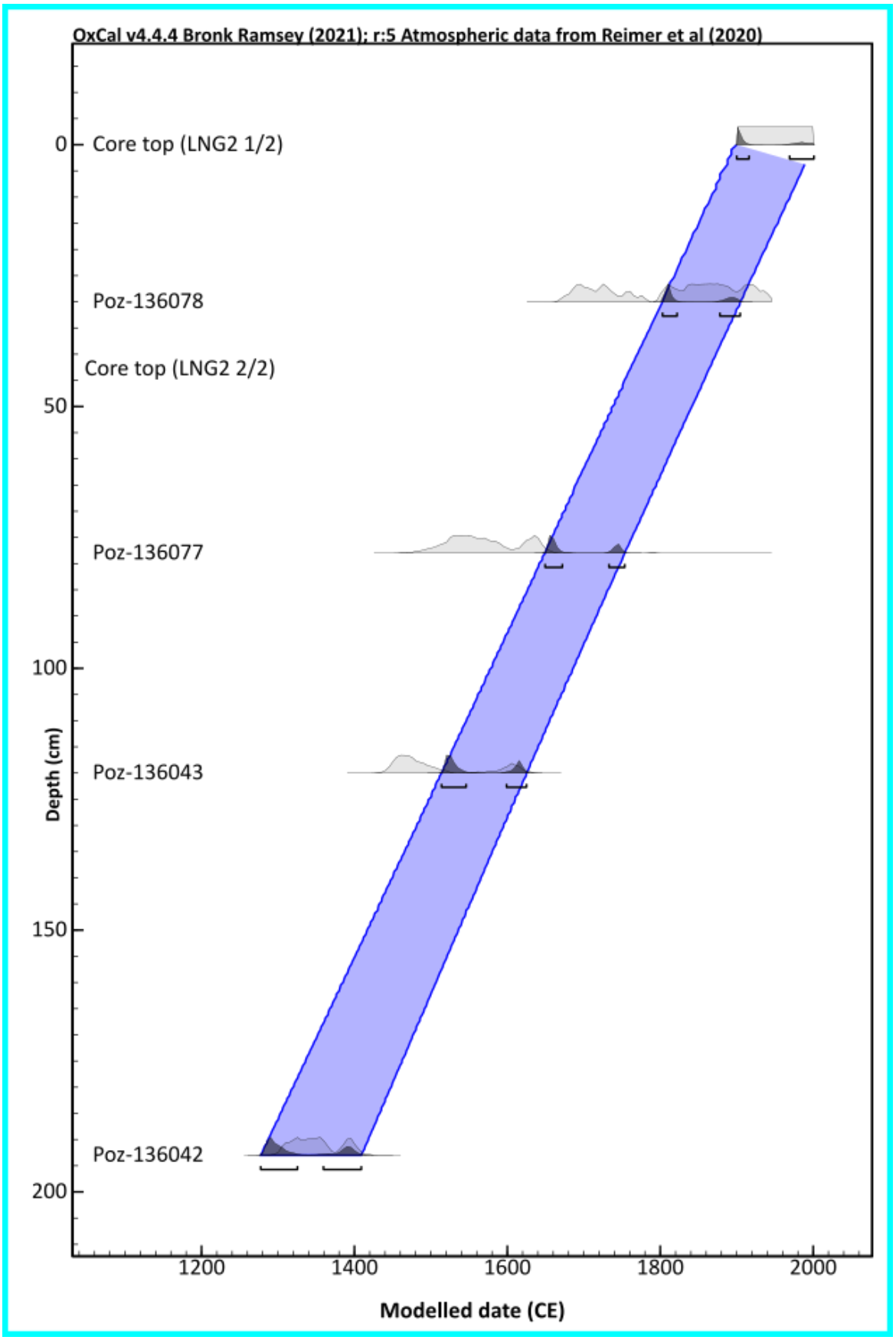

Figure 11: Age-Depth model using IntCal 20 based on Bronk Ramsey, 2021 applying Bayesian statistics methods (Bronk Ramsey, 2021).

4.5 Sedimentological Analysis

4.5.1 X-Ray Flourenscence (XRF)

In this thesis, Titanium (Ti), Incoherent, and Coherent ratio Inc/Coh have been used for analysis. Ti is being used in many research as a chemical proxy to link with increased rain and run-off (Corella et al., 2012), increased detrital input (Balascio et al., 2011), fine-grained detrital input (Martin-Puertas et al., 2012), silt rich facies (Yancheva et al., 2007). The variations in the intensity of titanium (Ti) can be utilized to identify the minerogenic influx and also can be used to infer the relationship between climate and the mineral influx (Martin-Puertas et al., 2012). The Compton (Incoherent) and Rayleigh (Coherent) ratio is mainly used for organic matter (Chawchai et al., 2016). The higher ratio of Inc/Coh indicates the presence of organic content (Burnett et al., 2011).

4.5.1.1 LNG1

LNG1 is one of the cores taken from Lagoa Negra Lake. All the cores were divided into five units (Figure 5). The LNG1 comprises 61.96cm in length. Units A, B, C, and D all comprise low values while Unit E shows the highest values of Ti (Figure 12). This suggests that there was a shift in sediment source and mineral input in the LNG1 core. The stable Inc/Coh values in Units D and E indicate that the organic matter content remained consistent despite the increase in minerogenic influx. The higher Ti values in Unit E suggest that there was a significant increase in weathering inputs, likely from a source that was rich in titanium. The variation in Ti values within Unit E, may indicate changes in the weathering intensity or the source of sediment over time. Overall, the results from LNG1 suggest that the LNG1 lake environment was influenced by changes in mineral input and sediment source, possibly driven by climatic changes.

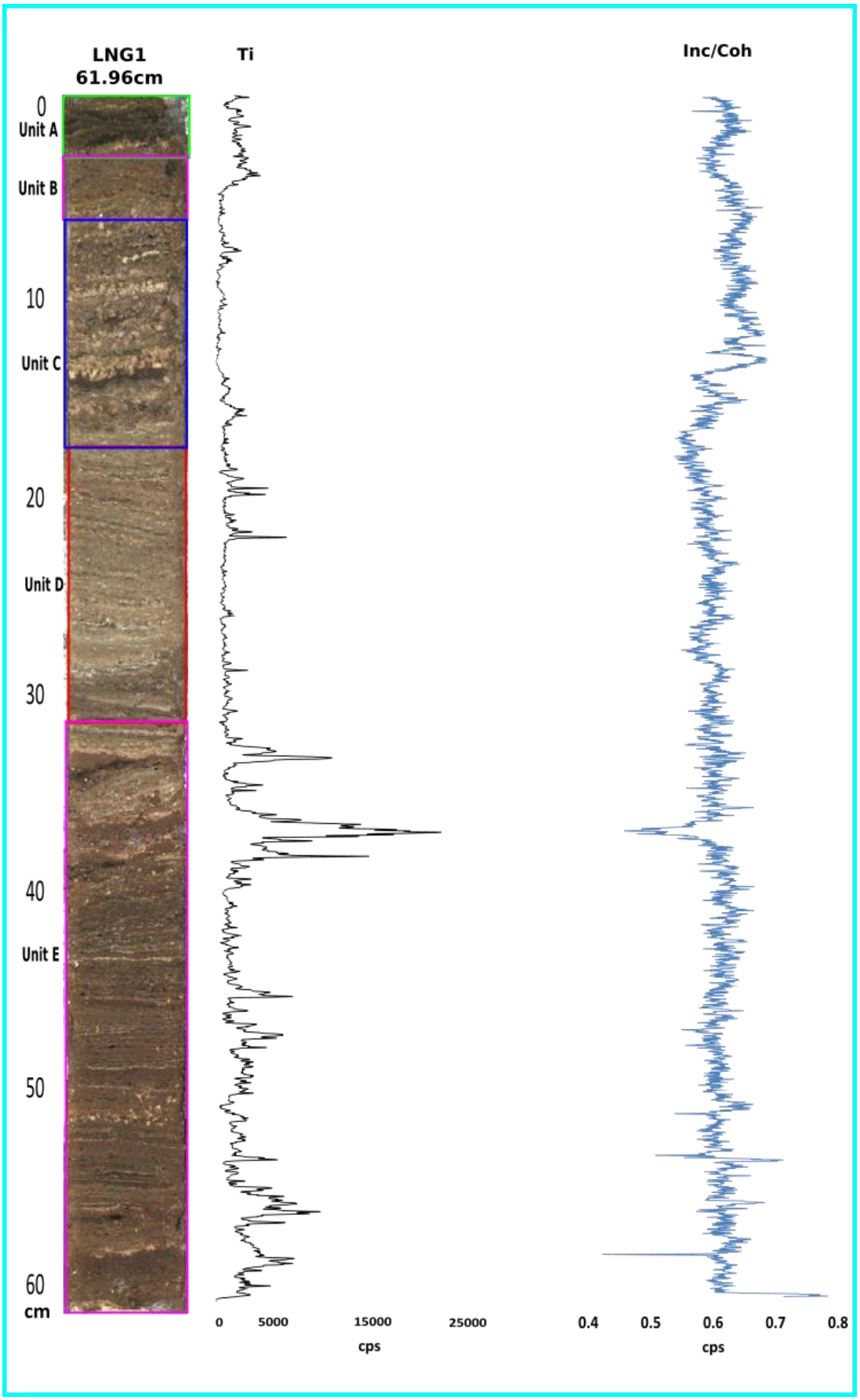

Figure 12: Correlation between A) sediment core LNG1 comprises 61.96cm in length B)Titanium Ti represents counts per second cps C) Incoherent Coherent Ratio Inc/Coh encompasses counts per second cps

4.5.1.2 LNG2 1/2

The LNG2 1/2 core overlaps and aligns with LNG1 as shown in Figure 5. The Ti behaved in LNG2 1/2 (Figure 13), as same as in LNG1 (Figure 12), which also happened with Inc/Coh. Both have been correlated, as can be seen in section 4.6.1. This suggests that the Ti concentration and minerogenic influx in the LNG2 1/2 core were similar to those observed in the LNG1 core, specifically in Unit E. The correlation between the Ti and Inc/Coh values in the two cores confirms that the sedimentary environment in LNG2 1/2 was similar to that in LNG1. The higher Ti values in Unit E of the LNG2 1/2 core suggest that the minerogenic influx was substantial, although slightly lower than in LNG1. The similarities between the two cores highlight the consistency of the sedimentary environment in the two parts of the lake and suggest that the climatic conditions that influenced the mineral input and sediment source were similar in both areas

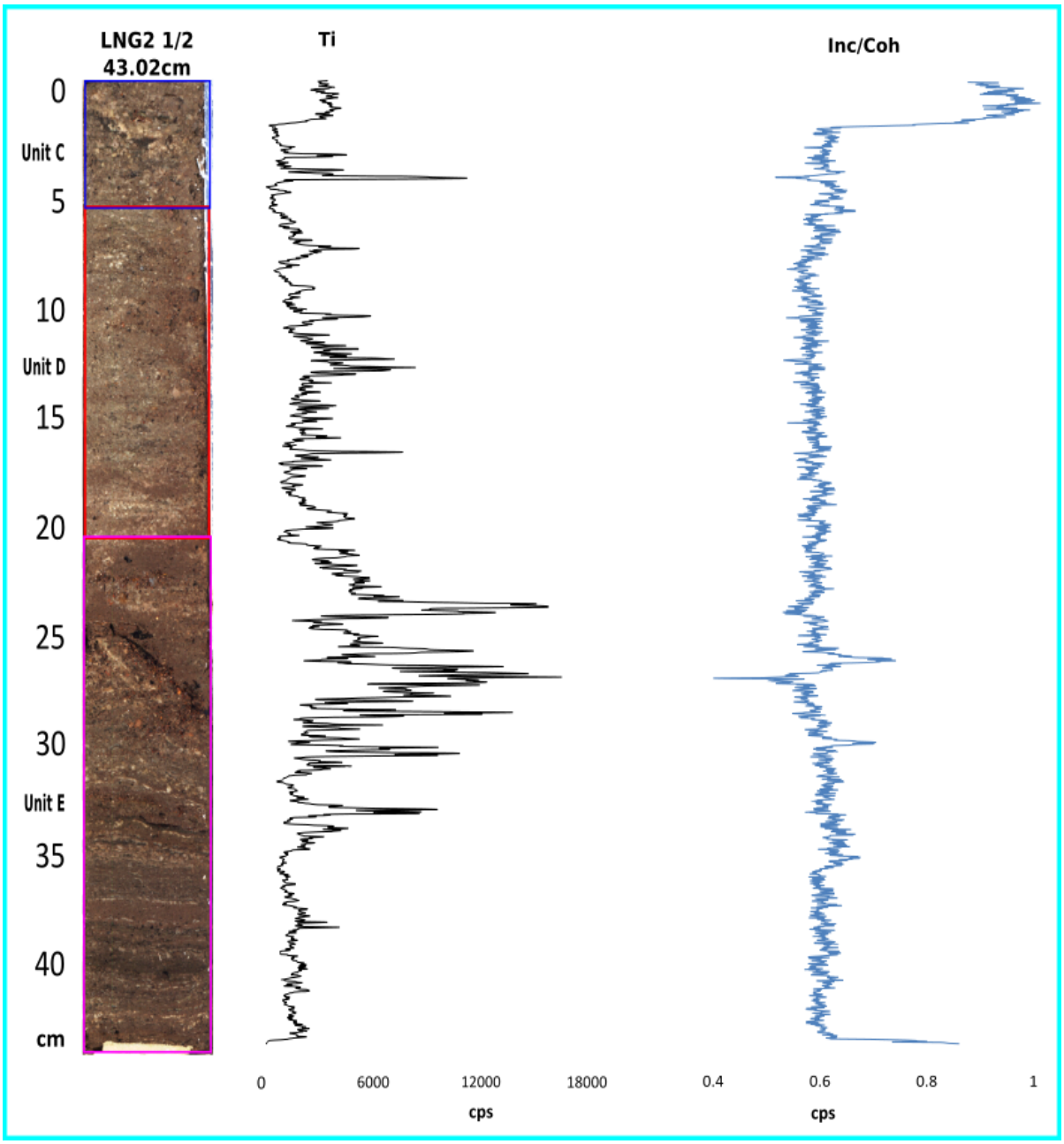

Figure 13: Correlation between A) sediment core LNG2 1/2 comprises 43.02cm in length B)Titanium Ti represents counts per second cps C) Incoherent Coherent Ratio Inc/Coh encompasses counts per second cps

4.5.1.3 LNG3

As LNG3 is aligned with LNG1 and LNG2 1/2 (Figure 5) replicates the same as the other two. This indicates that the sedimentary environment in the LNG3 core was similar to that in the LNG1 and LNG2 1/2 cores, with a high minerogenic influx observed in Unit D (Figure 14).

However, the Inc/Coh values in LNG3 show some variations compared to the other two cores, with higher values observed in Unit C. This difference in organic matter content may reflect variations in the depositional conditions or organic matter preservation in the different parts of

the lake. Overall, the results from LNG3 provide further evidence for the consistency of the sedimentary environment in the lake and suggest that the climatic conditions that influenced the mineral input and sediment source were similar in all three cores.

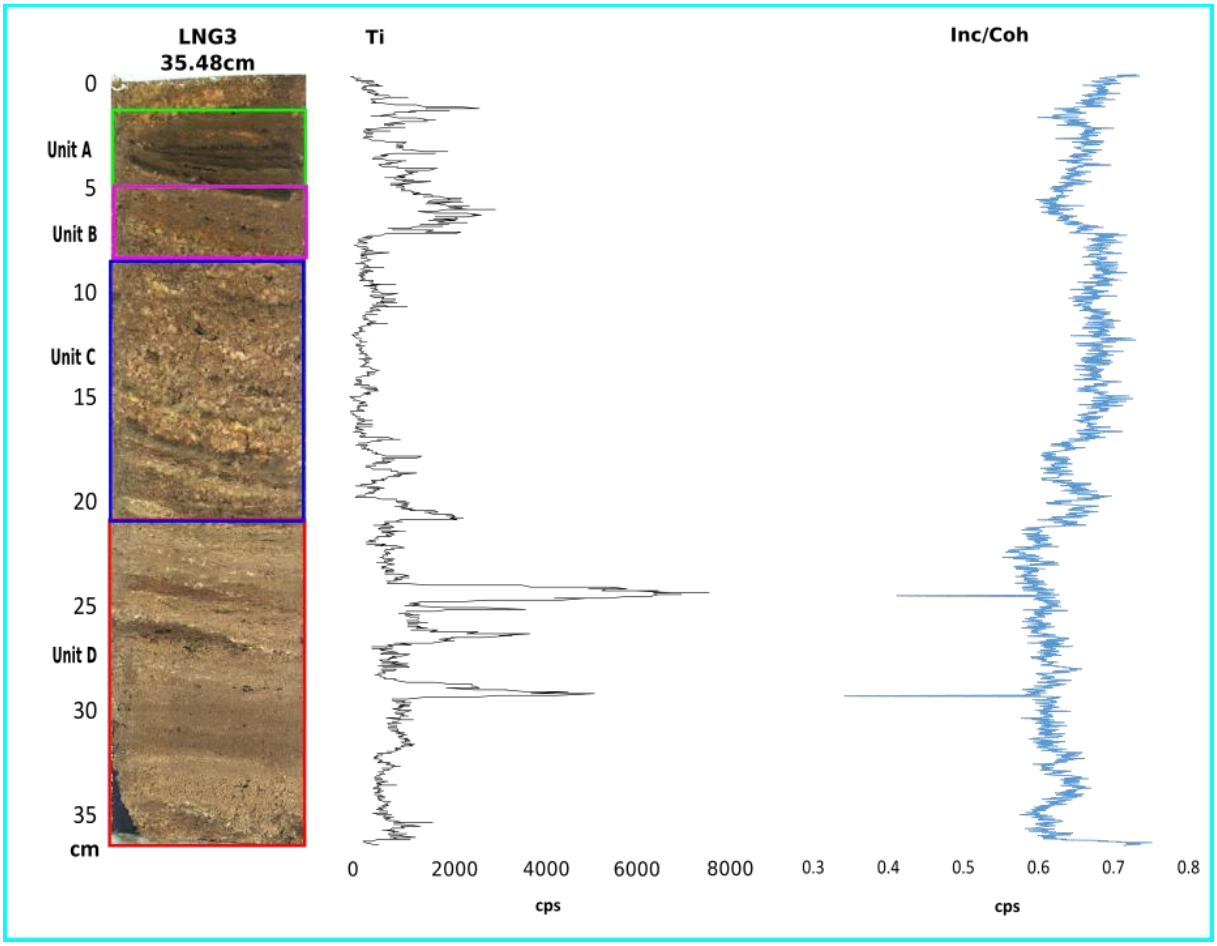

Figure 14: Correlation between A) sediment core LNG3 comprises 35.48cm in length B)Titanium Ti represents counts per second cps C) Incoherent Coherent Ratio Inc/Coh encompasses counts per second cps

4.5.1.4 LNG2 2/2

The LNG2 2/2 thoroughly shows the high peaks of Ti (Figure 15). This indicates that the sedimentary environment in the LNG2 2/2 core was characterized by the high minerogenic influx, with Ti values ranging from 5000 to 20000 cps. The high peaks in Ti suggest that the sediment source in this part of the lake was particularly rich in minerals. The stability of the Inc/Coh values suggests that the organic matter content remained consistent despite the high minerogenic influx. The zero values of Ti and Inc/Coh at 25cm may have been caused by physical damage to the sediment core, which disrupted the sediment record in this section. The high ratio of detrital input in the LNG2 2/2 core suggests that this part of the lake received a

substantial amount of sediment from external sources. Overall, the results from LNG2 2/2 highlight the variability of the sedimentary environment in the lake.

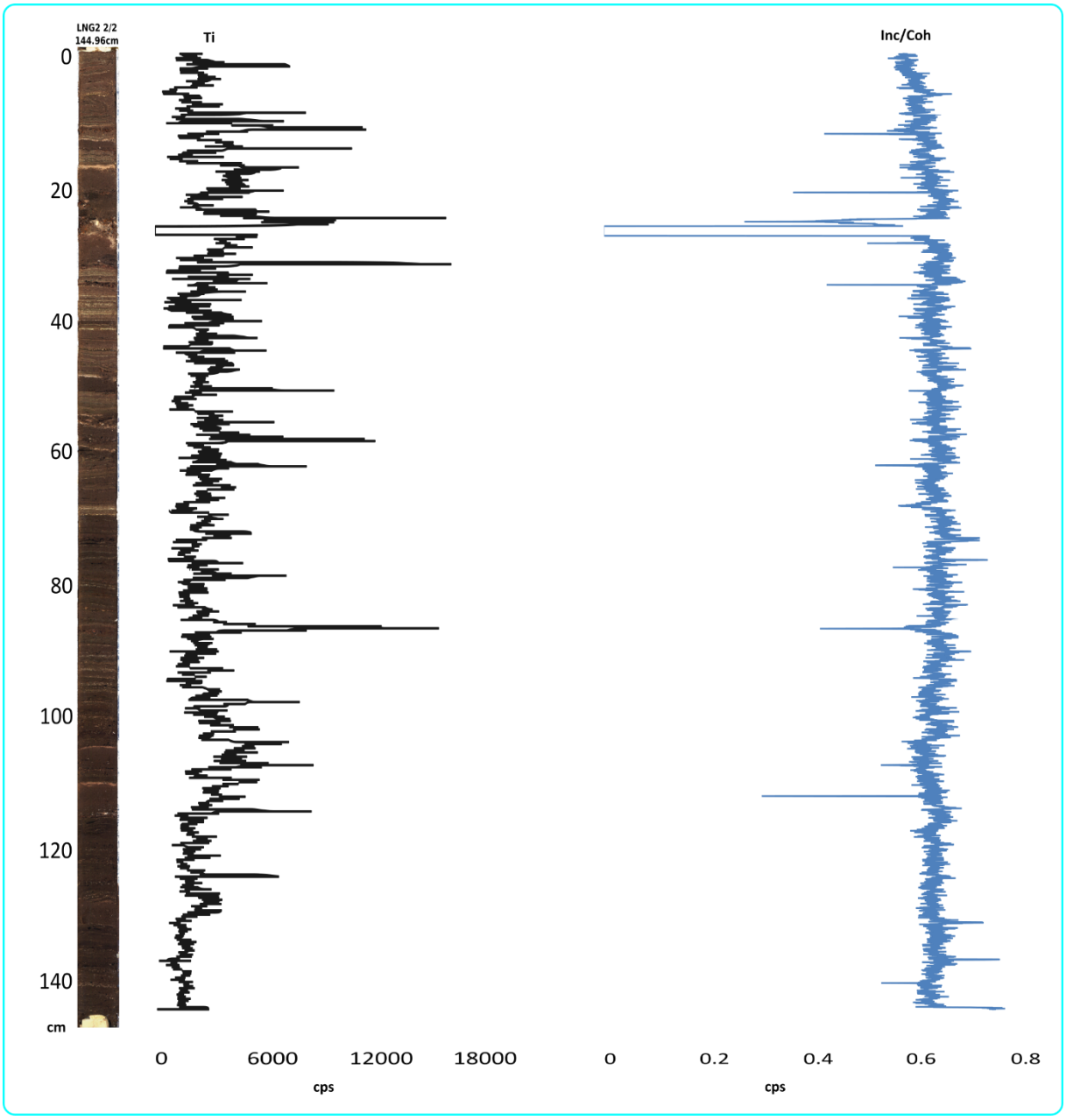

Figure 15: Correlation between A) sediment core LNG2 2/2 comprises 144.96cm in length B)Titanium Ti represents counts per second cps C) Incoherent Coherent Ratio Inc/Coh encompasses counts per second cps

4.6 Correlation:

All the cores have been extracted from the same lake Lagoa Negra, and the cores LNG1, LNG2 1/2, and LNG3 have a significant correlation to each other due to their similar lithology and aligned overlap (Figure 5). To see how positive they can be related to each other, QAnalySeries software is used, which can be used for time series tunning, analysis, and correlation. On the depth scale of LNG2 1/2, the other cores are correlated utilizing Ti. The LNG2 1/2 is correlated with LNG1 and LNG3, and LNG1 with LNG3.

4.6.1 LNG2 1/2 with LNG1

The correlation between LNG2 1/2 and LNG1 suggests that there is a strong similarity between the two cores in terms of their Ti content. This correlation is supported by the use of tie points during tuning, which helps to align the two cores on a depth scale. The strong positive correlation of 0.726 between LNG2 1/2 and LNG1(Figure 16) indicates that changes in Ti content in one core are closely reflected in the other. This high degree of correlation between the cores is a useful tool for understanding the relationship between the minerogenic influx and climate changes.

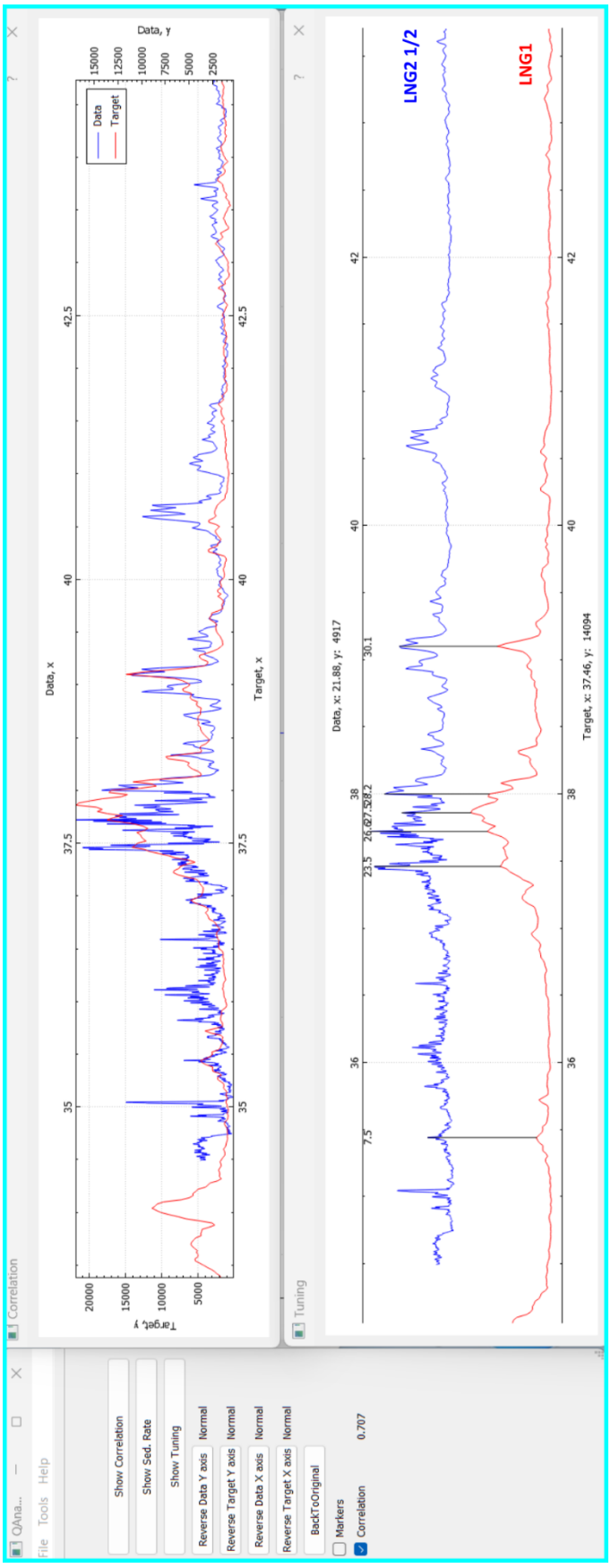

Figure 16: Correlation between LNG2 1/2, and LNG1 showing the positive reflection of 0.707. QAnalySeries is being used for interpretation. The blue line represents the Ti depth scale of sediment core LNG2 1/2, while the red line represents LNG1 comprises Ti values on the depth scale.

4.6.2 LNG1 and LNG3

The same procedure has been applied to LNG1 and LNG3. The relation of these has been positive and gives a correlation of 0.36 (Figure 17) This positive correlation implies that there is a consistent pattern of sedimentation and minerogenic influx in the lake over time.

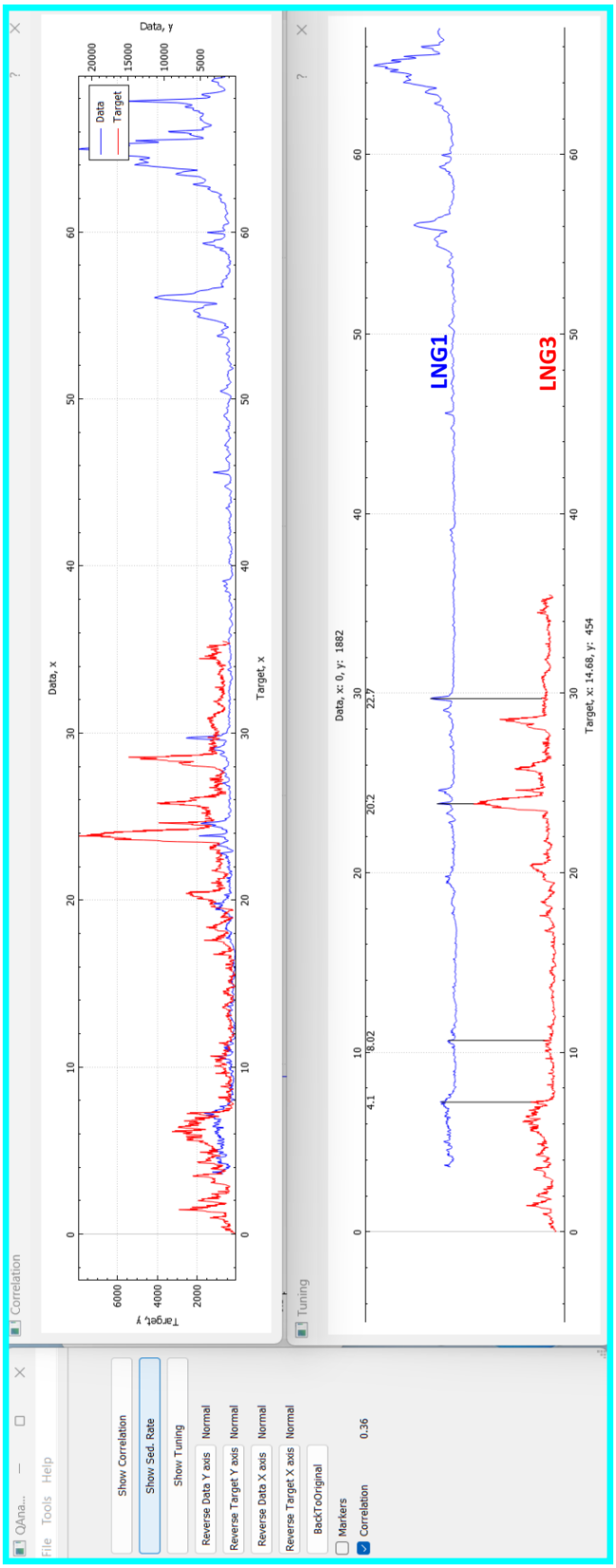

Figure 17: Correlation between LNG2 1/2, and LNG1 showing the positive reflection of 0.36. QAnalySeries is being used for interpretation. The blue line represents the Ti depth scale of sediment core LNG1, while the red line represents LNG3 comprises Ti values on the depth scale.

4.7 Hyperspectral Imaging Analysis

In the analysis of hyperspectral imaging data, the ENVI software package is utilized to perform spectral analysis on the Region of Interest (ROI). This process involves several steps to reduce the dimensionality of the data and extract endmembers, which represent the unique spectral signatures of different materials present in the ROI.

According to (Butz et al., 2015) the first step involves transforming the data using the minimum noise fraction (MNF) transformation and the pixel purity index (PPI). This helps in reducing the dimensionality of the data and removing noise and unwanted variability.

The next step involves cluster analysis, where the average spectra of different clusters are calculated. These average spectra are the endmembers of the spectral dataset, which represent the unique spectral signatures of different materials present in the ROI.

After extracting the endmembers, a classification method is applied to the data. The resulting post-classification spectral features are then examined, in this case, the absorption band from 950nm to 990nm.

4.7.1 Core LNG1

In Figure 18 part C, the blue color shows the temporal behavior sedimentation, which replicates the minerogenic influx with higher concentration, which can be aligned with the correspondence of Ti Figure 18 part B. The yellow color replicates the less detrital input and is corresponding with low values of Ti.

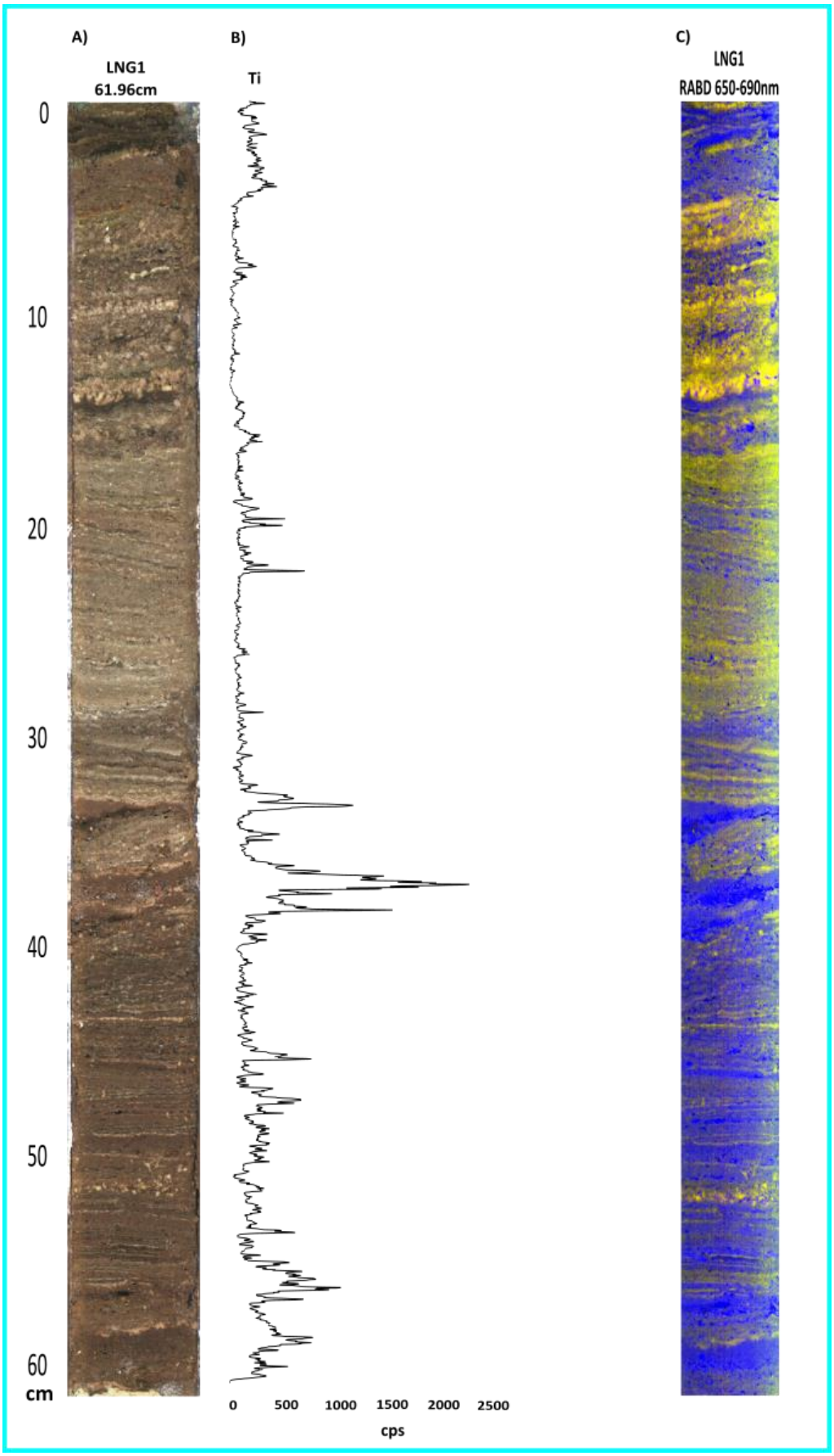

Figure 18: Schematics of A)LNG1 B)Ti count per seconds C) spectral classification profile comprising RABD 950-990nm

4.7.2 LNG2 1/2

As all the cores are extracted from the same lake Lagoa Negra giving the same temporal behavior. Figure 19 part B shows the correlation between the HSI and Ti results, where the higher the Ti value, the higher the minerogenic influx in the lake. In Figure 19 part C, the green color indicates higher detrital input compared to other areas, which is reflected in the higher values of Ti. On the other hand, the LNG2 1/2 core has low Ti values, which correspond to a low minerogenic influx in the lake.

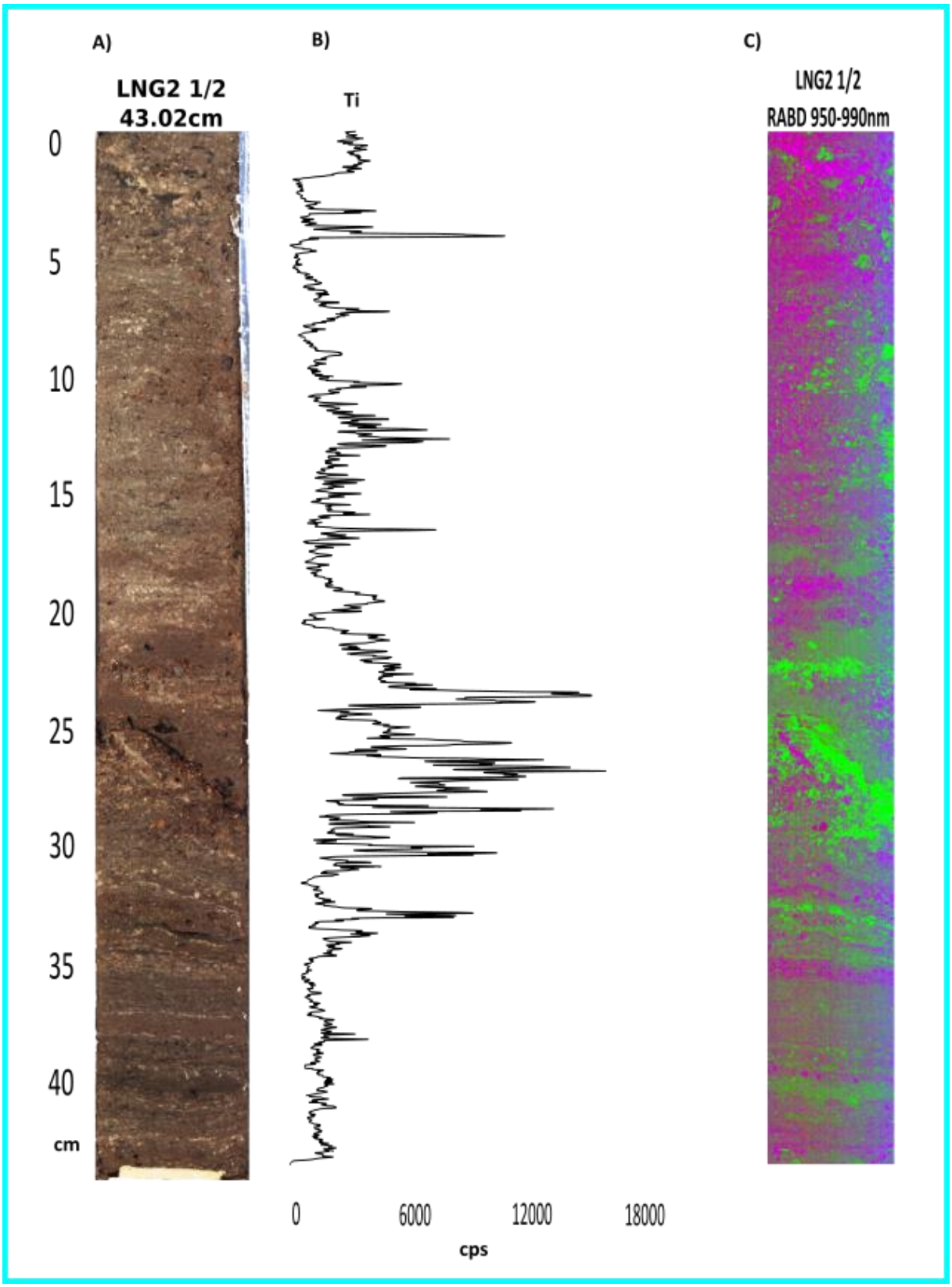

Figure 19: Schematics of A)LNG2 1/2 B)Ti count per seconds C) spectral classification profile comprising RABD 950-990nm

4.7.3 LNG3

The HSI analysis of LNG3 is also synchronized with the Ti values, as seen in Figure 20. The blue color in part C represents a higher intensity of detrital input, which aligns with the correspondence of Ti in part B. This confirms that the HSI analysis can accurately depict the sedimentation patterns and minerogenic influx in the cores, by analyzing the spectral data and correlating it with the Ti values.

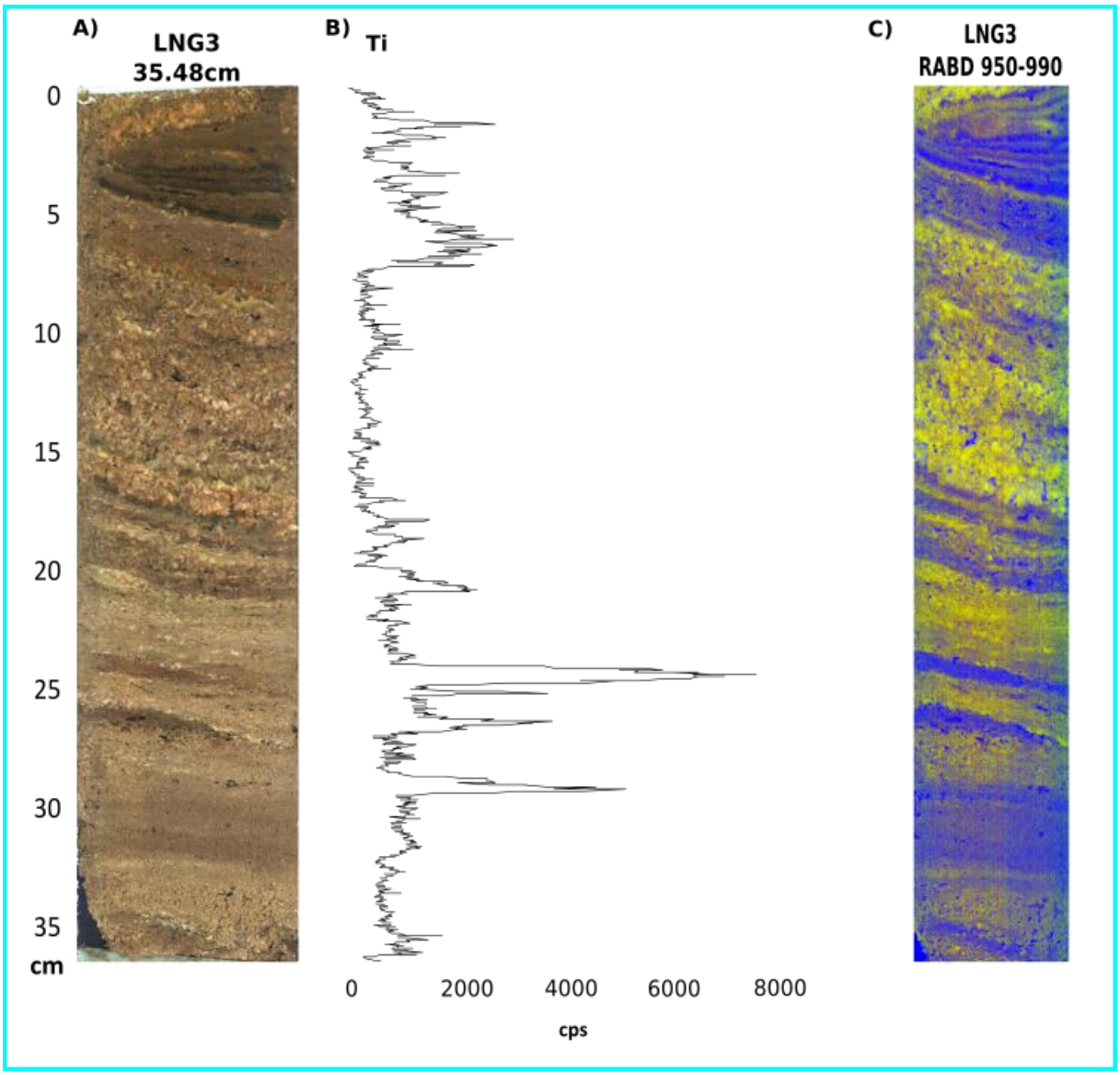

Figure 20: Schematics of A)LNG3 B)Ti count per seconds C) spectral classification profile comprising RABD 950-990nm

5 Discussion

5.1 Age Model

According to radiocarbon dating (Table 2) the Lagoa Negra lake sediment record leads to 1291 CE-1395 CE (last calibrated age from LNG2 2/2) of sediment accumulation, which corresponds to the late Holocene. Radiocarbon dating is considered to be not perfect, as it can give several errors which can be related to different impacts, such as fossil fuel, and bombing. The burning of fossil fuels releases large amounts of carbon dioxide into the atmosphere, which can affect the ratio of carbon-14 to carbon-12 in the atmosphere and cause the radiocarbon ages to appear older, also Nuclear weapons testing releases large amounts of carbon-14 into the atmosphere, which can cause the radiocarbon ages to appear younger than they appear to be (Hajdas et al., 2021). Furthermore, the contamination of the samples can also generate errors in radiocarbon dates. Adding old carbon of 1% to the sample may fluctuate the radiocarbon dates to hundreds of years (Walker, 2005). Due to said factors that can affect the amount of carbon-14 in the atmosphere, the radiocarbon ages must be calibrated to a curve based on measurements of carbon-14 from samples of known age. The calibrated radiocarbon age is then referred to as the calendar ages counted backward from 1950 CE (cal BP) or to calendar years before and within Common Era (BCE/CE). To produce the most accurate representation of past atmospheric carbon-14, IntCal radiocarbon calibration curves (Figure 11) are used (Hajdas et al., 2021).

5.2 Correlation between XRF and sediment stratigraphy

The purpose of this research is to reconstruct paleoclimate variability with a focus on the minerogenic influx. Four sediment cores from Lagoa Negra Lake Azores have been analyzed using high-resolution XRF and hyperspectral imaging methods.

All the cores are extracted from Lagoa Negra Lake. The LNG1, LNG2 1/2, and LNG3 have been lined up and aligned because they share the same lithology as shown in Figure 5. Furthermore, the cores are divided into five units. Unit A exhibits LNG1 and LNG3, which comprise a small portion of the cores. The Ti does not show that much high values, which can be considered normal minerogenic influx (Balascio et al., 2011). On the other hand, Inc/Coh also does not show any high influx of organic matter. Unit B exhibits LNG1 and LNG3. Which is again a small portion giving little high values and peak for Ti and less values for Inc/Coh could be a sign of low precipitation. Unit C covers all the cores LNG1, LNG2 1/2, and LNG3 showing very less values for Ti and high values of Inc/Coh, which could be interpreted as low minerogenic input and more organic matter. This unit can be considered as near to no

precipitation occurred. Unit D comprises all the cores, which show a small increase for Ti in the beginning, and then show very small values, which can be interpreted as low detrital input in the beginning and almost no sign of the minerogenic influx. Unit E comprises LNG1 and LNG2 1/2. In Figure 12 and Figure 13, it can be seen that unit E exhibits an abrupt change, which replicates the 1800 calibrated age (Figure 22). The Ti shows the highest peaks and values replicates up to 25000 cps, it can be said that unit E received more minerogenic influx and show a high intensity (Marshall et al., 2012). Which can be corresponding to the high intensity of the precipitation. While the Inc/Coh shows a normal trend except in one place.

The high percentage of sand in LNG1 (Figure 7) and the high percentage of silt in LNG2 1/2 (Figure 8) suggest different energy levels and sediment supply mechanisms in each location. For example, the presence of a higher amount of sand in LNG1 could indicate a depositional environment with higher energy levels, potentially due to stronger water flow could be due to precipitation. On the other hand, the higher silt content in LNG2 1/2 could be indicative of a depositional environment with weaker water flow or less wind, resulting in finer sediment particles being deposited.

LNG2 2/2 is the deepest sediment core of all cores and it is the continuation of LNG2 1/2 (Figure 22). Figure 15 shows that LNG2 2/2 exhibits high values of Ti which leads to 20000 cps, which is a continuation of unit E in LNG1 and LNG2 1/2, it can be observed that the high intensity of minerogenic influx continues, which may comprise high precipitation. Out of four samples, three samples were taken from LNG2 2/2 (Table 2) comprising calibrated years from 1291-1395 CE to 1664-1762 (Figure 11), so it can be believed that high precipitation intensities phases (Rothwell, 2015) have been observed in LNG2 2/2

Titanium can be used to infer changes in erosion and sedimentation patterns. For example, higher titanium concentrations in a sediment core may indicate that the area was experiencing increased erosion and sedimentation, possibly as a result of changes in precipitation or vegetation cover (Martin-Puertas et al., 2012).

The fine laminations observed in LNG2 2/2 (Figure 9) suggest that the sedimentation in this part of the lake was influenced by regular and consistent changes in sediment supply, water flow, and environmental conditions. The light yellowish to dark brown color of the sediment indicates that there was a varying input of minerals into the lake over time. The higher sand content (62.6%) in comparison to silt (37.4%) (Figure 10) suggests that there was relatively high energy in the depositional environment, potentially caused by wind, water currents, or other geological processes. The observation of lamination patterns in the upper portion of the

core being lighter in color than the lower portion could indicate changes in the intensity and frequency of these processes over time.

Although precipitation controls runoff, the relationship between titanium (as a proxy) and precipitation (as a climate variable) is not fully direct in the case of a lake. This is because various physical, chemical, and biological processes in lakes can transform the input forcing variable, such as precipitation, into something other than a simple output recording. For example, in the specific case of a lake, fluctuations in lake level caused by precipitation and variations in stream inflow can affect the distribution of detrital material within the lake. During episodes of increased precipitation, runoff, and lake level may also be higher, which would result in a greater influx of sediments into the lake, and thus higher titanium concentrations (Cohen, 2003). Overall, the LNG2 2/2 sediment core provides valuable information on the sediment composition, depositional environment, and historical changes that have taken place in the area.

5.3 Hyperspectral Imaging Spectroscopy:

Direct in-situ measurements employing spectroscopic techniques and reflectance in the VNIR range on fresh sediment cores have been successfully and routinely utilized for the investigation of the lake and ocean sediments. Attributing the spectral characteristics of lake sediments, such as their indices and endmembers, to particular elements in the sediment matrix continues to be a difficult task. Many organic and inorganic materials can be found in lake sediments, which all affect the spectrum reflectance (i.e., mixing of spectral signals). It has been observed that the absorption band occurs on specific substances and cases. The method used for calculating spectral indices is crucial, and the choice should be made with care. Pigment concentrations can be determined by using either Reflectance Absorption Band Depth (RABD) or Relative Absorption Band Areas (RABA). Whichever method is used, the choice of which bands to measure can have an impact on the outcome (Butz et al., 2015). In this research, RABD 950-990nm using endmember analysis and continuum removal has been analyzed. After calibration of RABD 950-990nm, it has been concluded that minerogenic influx may be retrieved from Hyperspectral data with an accuracy of 90%. Figures 18, 19, and 20 of LNG1, LNG 2 1/2, and LNG3 respectively show RABD 950-990nm plotted alongside XRF Ti showing the positive response.

5.4 Climate Implications

The use of Ti values in sediment records as a proxy for the minerogenic influx is can be used in the field of paleoclimate research. The presence of high values of Ti in the sediment cores is one of the indicators of the presence of minerogenic materials that have been deposited into the lake by various processes. It has been said that the layers with high values of Ti have been connected to precipitation. High values of the Ti, high would be the precipitation. To reconstruct the climate variability the Ti counts rates from XRF data have been used. The result is then compared with the studies and reconstructions of NAOOrtega (Ortega et al., 2015) and NAOTrouet (Trouet et al., 2009). The comparison of Ti (Figure 22) values with the North Atlantic Oscillation Index (NAOI) over the last millennium (Figure 21) provides an important tool for investigating past climate variability. The NAOI is a measure of the fluctuations in atmospheric pressure in the North Atlantic region and is a well-established proxy for climate variability (Rothwell, 2015). By comparing the Ti values in the sediment cores with the NAOI, it may gain insights into the relationship between climate and the mineral influx, which can provide important information about the environmental and climatic conditions that have shaped the landscape over time.

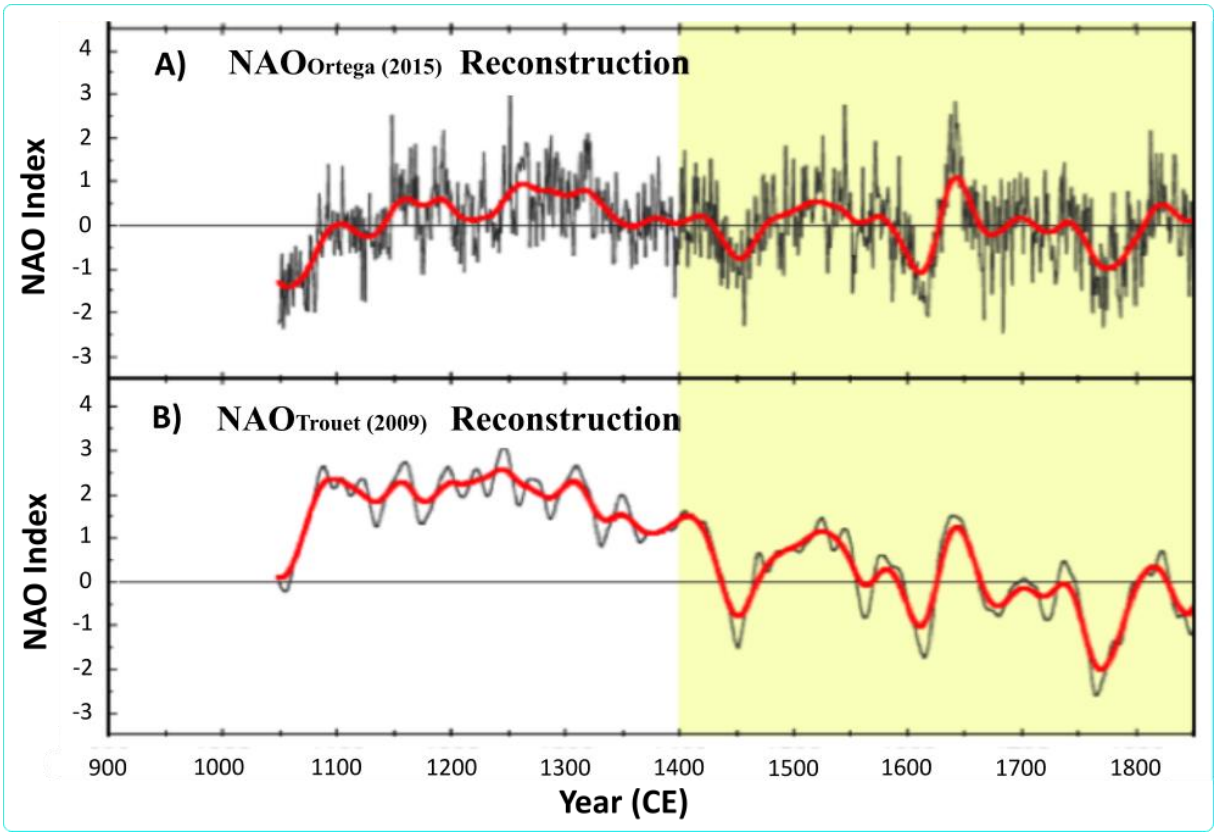

Figure 21: Comparing different NAO reconstructions A) NAOOrtega (Ortega et al., 2015) B) NAOTrouet (Trouet et al., 2009). The black line of each reconstruction has been smoothed with 50 years filter. The red line shows the NAO variability (Langnæs, 2019).

In LNG2 from 187cm to 150cm represents the calibrated age from 1290 to 1400 Figure 22, replicates the low Ti values, which can be assumed to be low precipitation. This agrees with the drier and stable conditions on Flores Island before 1400 CE (Richter et al., 2022). This is consistent with the findings of Ortega et al. (2015) and Trouet et al. (2009), who suggested that NAOI is positive and experienced dry and stable conditions before 1400 CE (Figure 21).

The study by Björck et al. (2006) and Richter et al. (2022) suggests that Flores Island experienced a prolonged wet period with high precipitation levels from 1400 CE to 500 CE. This is reflected in the sediment core LNG2/2, which shows a 150cm to 120cm section with increasing titanium values, indicating high minerogenic influx and high precipitation rates. The maximum Ti values comprise at a depth of 140cm representing 1450CE, which reaches out to 18000cps. Other than this shows normal behavior comparatively, and could be assumed as low precipitation. The NAO_{Ortega} and NAO_{Trouet} reconstructions support this finding, as they show this period as having a negative North Atlantic Oscillation Index (NAOI), which is associated with increased precipitation levels in the region.

From 1500 CE to 1600 CE the results shows the average precipitation corresponds to average values of Ti representing 120cm-90cm on LNG2 2/2 and might replicate the minerogenic influx (Figure 23), this result is not fully consistent with the finding of (Björck et al., 2006), where it has been said that at this phase NAO was negative and was experienced fairly high precipitation. However, there appears to be a conflict between NAO_{Ortega} and $NAO_{Trouet.}$, NAO_{Trouet} shows considerably dry weather while NAO_{Ortega} shows mild and wet weather.

From 90cm to 60cm of sediment core LNG2 2/2, the Ti counts give considerably high values, which could be a sign of high precipitation and minerogenic deposition. This part replicates the calibrated age from 1600 to 1700. Both NAO_{Ortega} and $NAO_{Trouet.}$ shows equal results in this time frame. It can be seen in Figure 21, from 1600 CE to 1630 CE, both the NAO_{Ortega} and NAO_{Trouet} reconstructions indicate a negative NAO, which is consistent with the findings of this research on precipitation levels on Flores Island during this time period. However, from 1630 CE to 1680 CE, the NAO_{Ortega} and NAO_{Trouet} reconstructions show a positive NAO, which is not in agreement with the research's findings. After 1680 CE, both the NAO_{Ortega} and NAO_{Trouet} reconstructions once again align with the study, indicating a negative NAO that corresponds to high precipitation levels on Flores Island. According to (Björck et al., 2006) 1600s CE is a high precipitation period, especially around 1650 CE, which represents NAO negative phrase, which is corresponding to this research. From 1700 CE to 1800 CE NAO_{Ortega} and NAO_{Trouet} represent the negative NAO and high precipitation and is not correspond to low values of Ti counts from 1700 CE to 1800CE as shown in Figure 22. In the early 1800s Figure 21 NAO_{Ortega} and Ti,

counts do not show good agreement. Ti shows high values which replicate high precipitation while NAO_{Ortega} shows a positive NAO. But according to (Björck et al., 2006) the early 1800s has a negative NAO and high precipitation, and positive NAO from 1850CE to 1870.

The grain size analysis also replicates the said discussion, as the average sedimentation of LNG2 2/2 comprises silty sand (Figure 10), which corresponds to the high values of Ti and high precipitation because the high precipitation could be medium of coarser sediments deposition because of its intensity. On the other hand, the LNG2 1/2, comprises sandy silt (Figure 8), which could be of low intensity of water flow and low precipitation.

It is important to note that while the reconstructed values of the North Atlantic Oscillation (NAO) in Figure 22 may show trends, they do not necessarily explain weather conditions in the Azores region, particularly on individual islands (Björck et al., 2006). However, there is a likelihood that the changes in the Figure reflect winter precipitation, which is often associated with changes in the larger-scale NAO.

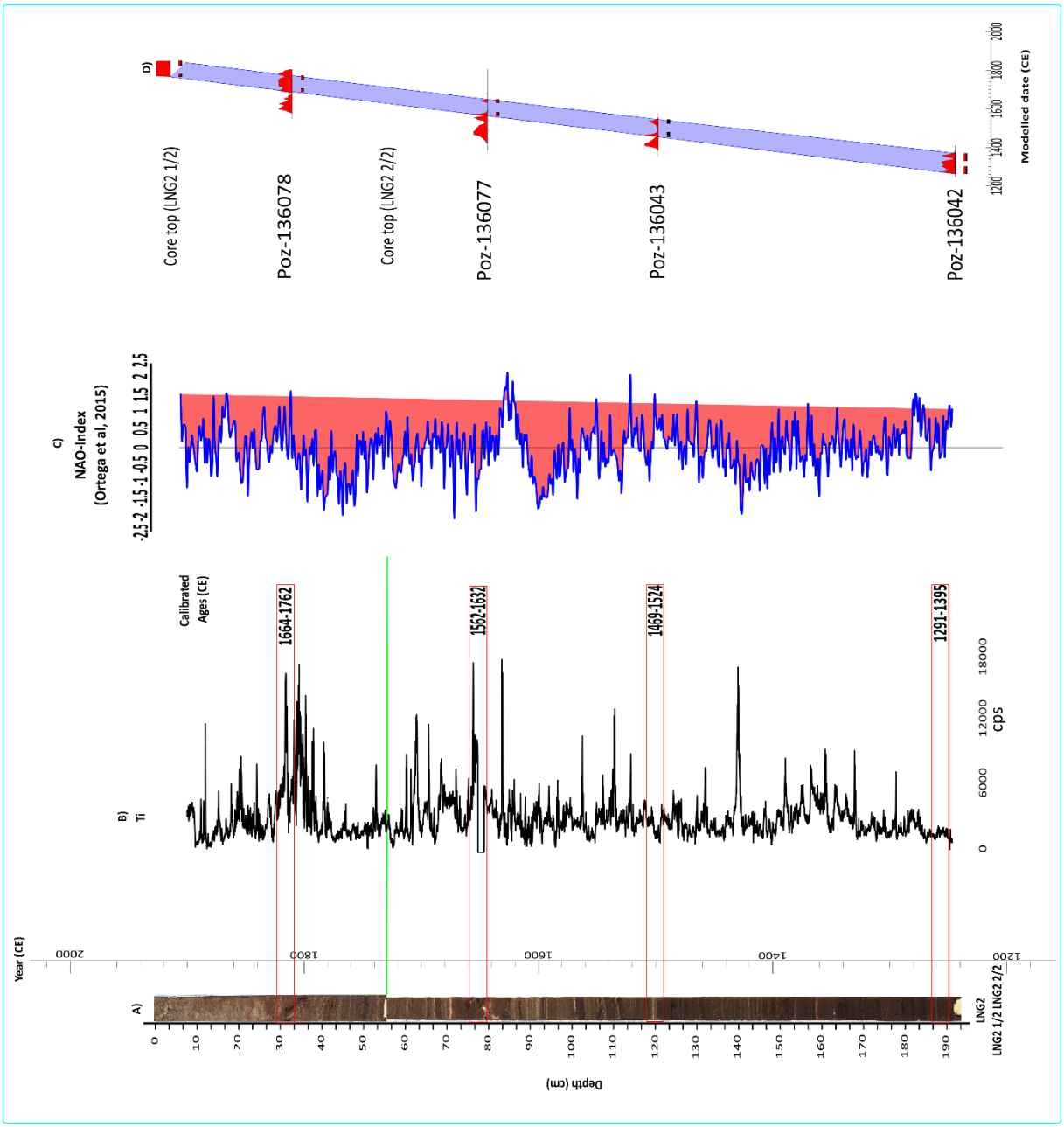

Figure 22: Comparing climate record A) LNG2 2/2 comprising 144.96cm B) Ti values in counts per second C) Inc/Coh ratio D) NAOOrtega (Ortega et al., 2015) E) Age model calibrated years CE

6 Conclusion:

The results, interpretation, and discussion of the Lagoa Negra Lake sediments analysis can be summarized as follows:

- Four sediment cores LNG1, LNG2 1/2, LNG3, and LNG2/2 has been analyzed for paleoclimate reconstruction
- The sediment composition of LNG1 is composed of silty sand with an average of 51.7% sand and 48.3% silt, while LNG2 1/2 is composed of sandy silt with 42.8% sand and 57.2% silt, The sedimentation in LNG2 2/2 is silty sand, with 62.6% sand and 37.4% silt, These sediment compositions provide valuable information about the depositional environment and processes that shaped the landscape.
- The use of radiocarbon dating calibration has provided an estimated age range for the sediments analyzed in the Lagoa Negra Lake, which is estimated to be between 1291-1395 CE to 1664-1762 CE.
- Units A to D of LNG1 and LNG2 2/2 have not shown any drastic change and replicated low Ti values, which cover the age from 1762 CE to the recent.
- Unit E of LNG1 and LNG2 1/2 show the shift in the gain of minerogenic influx corresponding to high values of Ti, this trend continues in LNG2 2/2 core as well, which might represent high precipitation representing 1261CE to 1762CE.
- The Inc/Coh values in the sediment cores remained relatively stable and followed a typical trend and not showed any extreme shift, which can be understood that there is no significant amount of organic matter influx.
- The RABD 950-990nm of hyperspectral imaging replicated the minerogenic influx linked to Ti peak values. The correlation between Ti peak values and the minerogenic influx indicates the significance of using hyperspectral imaging as a tool for mineral identification in sediment core analysis.
- From 1290 CE to 1400 CE low minerogenic influx corresponded to low precipitation could be a dry period and suggest positive NAO
- 1450CE replicates the high values of Ti, suggesting high minerogenic influx and precipitation, which could be negative NAO.
- From 1450CE to 1600CE no considerable high values are found and could be considered as low precipitation or positive NAO period.
- 1600CE to 1700CE the Ti values show some peaks and high values suggest that in period precipitation could be experienced.

- 1700CE to 1800CE low values of Ti may replicate the low precipitation or dry weather.

6.1 Future work

This thesis has been a thought-provoking and educational experience, providing a wealth of data that can be further analyzed. It is a stimulating field for continuing research in reconstructing the paleoclimate of Flores Island Azores

- First of all, It would have been beneficial to have additional exposure dating from the study area. This could have helped to analyze the sedimentation history of long periods and cover a larger period of climate variability
- A multi-disciplinary approach can be used that incorporates multiple lines of evidence and a wider range of methods to obtain a more robust understanding of the sedimentation history and paleoclimate of the region
- To strengthen the understanding of climate variability at Flores Island, it will be necessary to conduct further research on other lakes in the Azores.

References:

Adrian, R., O'Reilly, C. M., Zagarese, H., Baines, S. B., Hessen, D. O., Keller, W., Livingstone, D. M., Sommaruga, R., Straile, D., & Van Donk, E. (2009). Lakes as sentinels of climate change. *Limnology and oceanography*, *54*(6part2), 2283-2297.

Anderson, H. J., Moy, C. M., Vandergoes, M. J., Nichols, J. E., Riesselman, C. R., & Van Hale, R. (2018). Southern Hemisphere westerly wind influence on southern New Zealand hydrology during the Lateglacial and Holocene. *Journal of Quaternary Science*, *33*(6), 689-701.

Andrade, C., Trigo, R., Freitas, M., Gallego, M., Borges, P., & Ramos, A. (2008). Comparing historic records of storm frequency and the North Atlantic Oscillation (NAO) chronology for the Azores region. *The Holocene*, *18*(5), 745-754.

Andrade, M., Ramalho, R. S., Pimentel, A., Hernández, A., Kutterolf, S., Sáez, A., Benavente, M., Raposeiro, P. M., & Giralt, S. (2021). Unraveling the holocene eruptive history of Flores Island (Azores) through the analysis of lacustrine sedimentary records. *Frontiers in Earth Science*, 889.

Azevedo, J., & Ferreira, M. P. (2006). The volcanotectonic evolution of Flores Island, Azores (Portugal). *Journal of volcanology and geothermal research*, *156*(1-2), 90-102.

Báez, J. C., Gimeno, L., & Real, R. (2021). North Atlantic Oscillation and fisheries management during global climate change. *Reviews in Fish Biology and Fisheries*, *31*(2), 319-336.

Balascio, N. L., Zhang, Z., Bradley, R. S., Perren, B., Dahl, S. O., & Bakke, J. (2011). A multi-proxy approach to assessing isolation basin stratigraphy from the Lofoten Islands, Norway. *Quaternary Research*, *75*(1), 288-300.

Barr, C., Tibby, J., Gell, P., Tyler, J., Zawadzki, A., & Jacobsen, G. E. (2014). Climate variability in south-eastern Australia over the last 1500 years inferred from the high-resolution diatom records of two crater lakes. *Quaternary Science Reviews*, *95*, 115-131. https://doi.org/10.1016/j.quascirev.2014.05.001

Björck, S., Rittenour, T., Rosén, P., França, Z., Möller, P., Snowball, I., Wastegård, S., Bennike, O., & Kromer, B. (2006). A Holocene lacustrine record in the central North Atlantic: proxies for volcanic activity, short-term NAO mode variability, and long-term precipitation changes. *Quaternary Science Reviews*, *25*(1-2), 9-32.

Borges, P. A., Amorim, I. R., Cunha, R. T. d., Gabriel, R., Martins, A. M., Silva, L., Costa, A. C., & Vieira, V. (2009). Azores. *Encyclopedia of islands*, 70-75.

Boyle, J. F. (2000). Rapid elemental analysis of sediment samples by isotope source XRF. *Journal of Paleolimnology*, *23*(2), 213-221.

Bradley, R. S. (1999). *Paleoclimatology: reconstructing climates of the Quaternary*. Elsevier.

Burnett, A. P., Soreghan, M. J., Scholz, C. A., & Brown, E. T. (2011). Tropical East African climate change and its relation to global climate: a record from Lake Tanganyika, Tropical East Africa, over the past 90+ kyr. *Palaeogeography, Palaeoclimatology, Palaeoecology*, *303*(1-4), 155-167.

Butz, C., Grosjean, M., Fischer, D., Wunderle, S., Tylmann, W., & Rein, B. (2015). Hyperspectral imaging spectroscopy: a promising method for the biogeochemical analysis of lake sediments. *Journal of Applied Remote Sensing*, *9*(1). https://doi.org/10.1117/1.Jrs.9.096031

Chawchai, S., Kylander, M. E., Chabangborn, A., Löwemark, L., & Wohlfarth, B. (2016). Testing commonly used X-ray fluorescence core scanning-based proxies for organic-rich lake sediments and peat. *Boreas*, *45*(1), 180-189. https://doi.org/10.1111/bor.12145

Cohen, A. S. (2003). *Paleolimnology: the history and evolution of lake systems*. Oxford university press.

Connor, S. E., van Leeuwen, J. F., Rittenour, T. M., van der Knaap, W. O., Ammann, B., & Björck, S. (2012). The ecological impact of oceanic island colonization–a palaeoecological perspective from the Azores. *Journal of Biogeography*, *39*(6), 1007-1023.

Corella, J. P., Brauer, A., Mangili, C., Rull, V., Vegas-Vilarrúbia, T., Morellón, M., & Valero-Garcés, B. L. (2012). The 1.5-ka varved record of Lake Montcortès (southern Pyrenees, NE Spain). *Quaternary Research*, *78*(2), 323-332.

Croudace, I. W., Rindby, A., & Rothwell, R. G. (2006). ITRAX: description and evaluation of a new multi-function X-ray core scanner. *Geological Society, London, Special Publications*, *267*(1), 51-63.

Ekoa Bessa, A. Z., Armstrong-Altrin, J. S., Fuh, G. C., Bineli Betsi, T., Kelepile, T., & Ndjigui, P.-D. (2021). Mineralogy and geochemistry of the Ngaoundaba Crater Lake sediments, northern Cameroon: implications for provenance and trace metals status. *Acta Geochimica*, *40*(5), 718-738. https://doi.org/10.1007/s11631-021-00463-5

França, Z., Cruz, J. V., Nunes, J. C., & Forjaz, V. H. (2003). Geologia dos Açores: uma perspectiva actual. *Açoreana*, *10*(1), 11-140.

Genske, F. S., Beier, C., Stracke, A., Turner, S. P., Pearson, N. J., Hauff, F., Schaefer, B. F., & Haase, K. M. (2016). Comparing the nature of the western and eastern Azores mantle. *Geochimica et cosmochimica acta*, *172*, 76-92.

Hajdas, I., Ascough, P., Garnett, M. H., Fallon, S. J., Pearson, C. L., Quarta, G., Spalding, K. L., Yamaguchi, H., & Yoneda, M. (2021). Radiocarbon dating. *Nature Reviews Methods Primers*, *1*(1), 1-26.

Hernández, A., Sáez, A., Bao, R., Raposeiro, P. M., Trigo, R. M., Doolittle, S., Masqué, P., Rull, V., Gonçalves, V., & Vázquez-Loureiro, D. (2017). The influences of the AMO and NAO on the sedimentary infill in an Azores Archipelago lake since ca. 1350 CE. *Global and Planetary Change*, *154*, 61-74.

Hildenbrand, A., Marques, F., & Catalão, J. (2018). Large-scale mass wasting on small volcanic islands revealed by the study of Flores Island (Azores). *Scientific reports*, *8*(1), 1-11.

Hosseini, S. M., Kashki, A., & Karami, M. (2022). Analysis of the North Atlantic Oscillation Index and rainfall in Iran. *Modeling Earth Systems and Environment*, *8*(3), 3647-3656.

Hurrell, J. W., & Deser, C. (2010). North Atlantic climate variability: The role of the North Atlantic Oscillation. *Journal of Marine Systems*, *79*(3-4), 231-244. https://doi.org/10.1016/j.jmarsys.2009.11.002

Iqbal, M., & Rashid, S. F. (2016). A re-interpretation of impact of the Icelandic Low and Azores High on winter precipitation over Iberian Peninsula. *Arabian Journal of Geosciences*, *9*(2), 1-7.

Koetse, M. J., & Rietveld, P. (2009). The impact of climate change and weather on transport: An overview of empirical findings. *Transportation Research Part D: Transport and Environment*, *14*(3), 205-221.

Marshall, M., Schlolaut, G., Nakagawa, T., Lamb, H., Brauer, A., Staff, R., Ramsey, C. B., Tarasov, P., Gotanda, K., & Haraguchi, T. (2012). A novel approach to varve counting using µXRF and X-radiography in combination with thin-section microscopy, applied to the Late Glacial chronology from Lake Suigetsu, Japan. *Quaternary Geochronology*, *13*, 70-80.

Martin-Puertas, C., Brauer, A., Dulski, P., & Brademann, B. (2012). Testing climate–proxy stationarity throughout the Holocene: an example from the varved sediments of Lake Meerfelder Maar (Germany). *Quaternary Science Reviews*, *58*, 56-65.

Mason, R. P., Fitzgerald, W. F., & Morel, F. M. (1994). The biogeochemical cycling of elemental mercury: anthropogenic influences. *Geochimica et cosmochimica acta*, *58*(15), 3191-3198.

Métrich, N., Zanon, V., Créon, L., Hildenbrand, A., Moreira, M., & Marques, F. O. (2014). Is the 'Azores hotspot'a wetspot? Insights from the geochemistry of fluid and melt inclusions in olivine of Pico basalts. *Journal of Petrology*, *55*(2), 377-393.

Meyers, P. A., & Lallier-Vergès, E. (1999). Lacustrine sedimentary organic matter records of Late Quaternary paleoclimates. *Journal of Paleolimnology*, *21*(3), 345-372.

Nguetsop, V. F., Bentaleb, I., Favier, C., Bietrix, S., Martin, C., Servant-Vildary, S., & Servant, M. (2013). A late Holocene palaeoenvironmental record from Lake Tizong, northern Cameroon using diatom and carbon stable isotope analyses. *Quaternary Science Reviews*, *72*, 49-62.

Ortega, P., Lehner, F., Swingedouw, D., Masson-Delmotte, V., Raible, C. C., Casado, M., & Yiou, P. (2015). A model-tested North Atlantic Oscillation reconstruction for the past millennium. *Nature*, *523*(7558), 71-74.

Pinto, J. G., & Raible, C. C. (2012). Past and recent changes in the North Atlantic oscillation. *Wiley Interdisciplinary Reviews: Climate Change*, *3*(1), 79-90.

Powers, L. A., Werne, J. P., Johnson, T. C., Hopmans, E. C., Sinninghe Damsté, J. S., & Schouten, S. (2004). Crenarchaeotal membrane lipids in lake sediments: A new paleotemperature proxy for continental paleoclimate reconstruction? *Geology*, *32*(7). https://doi.org/10.1130/g20434.1

Rein, B., & Sirocko, F. (2002). In-situ reflectance spectroscopy–analysing techniques for high-resolution pigment logging in sediment cores. *International Journal of Earth Sciences*, *91*(5), 950-954.

Richter, N., Russell, J. M., Amaral-Zettler, L., DeGroff, W., Raposeiro, P. M., Gonçalves, V., de Boer, E. J., Pla-Rabes, S., Hernández, A., & Benavente, M. (2022). Long-term hydroclimate variability in the sub-tropical North Atlantic and anthropogenic impacts on lake ecosystems: A case study from Flores Island, the Azores. *Quaternary Science Reviews*, *285*, 107525.

Rodrigues, F., & Antunes, P. (2014). Hydrogeochemistry assessment of volcanic lakes in the Flores Island protected areas (Azores, Portugal). *Revista de Gestão Costeira Integrada-Journal of Integrated Coastal Zone Management*, *14*(2), 321-334.

Rothwell, R. G. (2015). Twenty years of XRF core scanning marine sediments: What do geochemical proxies tell us? In *Micro-XRF studies of sediment cores* (pp. 25-102). Springer.

Ryżak, M., & Bieganowski, A. (2011). Methodological aspects of determining soil particle-size distribution using the laser diffraction method. *Journal of Plant Nutrition and Soil Science*, *174*(4), 624-633.

Santos, R. S., Hawkins, S., Monteiro, L. R., Alves, M., & Isidro, E. J. (1995). Marine research, resources and conservation in the Azores. *Aquatic Conservation: Marine and Freshwater Ecosystems*, *5*(4), 311-354.

Sarachik, E., Alverson, K., & IPO, P. (2000). Opportunities for CLIVAR/PAGES NAO Studies. *PAGES Newsletter*, *8*(1), 14-16.

Shippert, P. (2003). Introduction to hyperspectral image analysis. *Online Journal of Space Communication*, *2*(3), 8.

Trouet, V., Esper, J., Graham, N. E., Baker, A., Scourse, J. D., & Frank, D. C. (2009). Persistent positive North Atlantic Oscillation mode dominated the medieval climate anomaly. *science*, *324*(5923), 78-80.

Van Exem, A., Debret, M., Copard, Y., Vannière, B., Sabatier, P., Marcotte, S., Laignel, B., Reyss, J.-L., & Desmet, M. (2018). Hyperspectral core logging for fire reconstruction studies. *Journal of Paleolimnology*, *59*(3), 297-308.

Walker, M. (2005). *Quaternary dating methods*. John Wiley and Sons.

Wanner, H., Brönnimann, S., Casty, C., Gyalistras, D., Luterbacher, J., Schmutz, C., Stephenson, D. B., & Xoplaki, E. (2001). North Atlantic Oscillation–concepts and studies. *Surveys in geophysics*, *22*(4), 321-381.

Yancheva, G., Nowaczyk, N. R., Mingram, J., Dulski, P., Schettler, G., Negendank, J. F., Liu, J., Sigman, D. M., Peterson, L. C., & Haug, G. H. (2007). Influence of the intertropical convergence zone on the East Asian monsoon. *Nature*, *445*(7123), 74-77.

Zander, P. D., Wienhues, G., & Grosjean, M. (2022). Scanning Hyperspectral Imaging for In Situ Biogeochemical Analysis of Lake Sediment Cores: Review of Recent Developments. *Journal of imaging*, *8*(3), 58.